UNIVERSITÀ
DEGLI STUDI
FIRENZE

DOTTORATO DI RICERCA IN
PROGETTO E SVILUPPO DI PRODOTTI E
PROCESSI INDUSTRIALI

Car Body Concept Modeling: Congruency Equations for Hybrid Structures

Alessio Moroncini

UNIVERSITÀ
DEGLI STUDI
FIRENZE

DOTTORATO DI RICERCA IN PROGETTO E SVILUPPO DI PRODOTTI E PROCESSI INDUSTRIALI

CICLO XXV

Car Body Concept Modeling: Congruency Equations for Hybrid Structures

Settore Scientifico Disciplinare ING/IND 14

Candidato
Ing. Alessio Moroncini

Tutore
Prof. Niccolò Baldanzini

Controrelatore
Prof. Domenico Mundo

Coordinatore del Dottorato
Prof. Marco Pierini

Anni 2010/2014

“You don't write because you want to say something; you write because you've got something to say” F. S. Fitzgerald

Abstract

The aim of this PhD thesis is to define a set of congruency equations for the rigorous connection of dissimilar FEM elements for hybrid thin-walled structures, whereby one-dimensional elements are coupled with three-dimensional joint structures.

The set of congruency equations defined within the framework of this research activity has been applied in the field of automotive concept modeling.

The first part of the thesis concerns with an introduction to the car body concept modelling method for the early design phase of the “Body in White” with a special focus on NVH structural optimization and “hybrid modeling” techniques.

The second part of the thesis relates to the definition of the connecting equations for the hybrid structures through the “principle of virtual work” and a fundamental property of the center of mass of cross sections defined by the author within this dissertation.

Finally a validation phase of the congruency equations for hybrid structures and the integration of a hybrid model in a multi-objective optimization sequence, is presented.

Contents

1 INTRODUCTION

The continuous research activity on high performance simulation models and methods, seeking for an always higher accuracy and reliability, has driven this study towards the definition of a set of congruency equations for the rigorous connection of dissimilar FEM elements for concept modeling applications. In this first chapter, the background, the aim of this work and an introduction to the "vehicle concept modeling" methodology for car body design, context of this work, is described.

1.1 Background and aim of the work

The present research activity has been fully endorsed by the European Commission through a Marie Curie Action. The project, "VEhicle Concept Modeling" (VECOM), has been joined by 14 academic and industrial partners across Europe with the aim of providing dedicated research activities and trainings in the emerging field of vehicle concept modelling for up-front pre-CAD functional performance engineering, bridging between industry and academia. In particular this dissertation has been developed at BMW Group in Munich, Germany (acting as host organization), under the academic supervision of the University of Florence, Italy. The "vehicle concept modeling" research area is of highly strategic importance to European automotive OEMs, who must launch products on an ever shorter time frame, at increased quality of multiple performance attributes. When simulation results become available in an early design stage, problems can already be solved before the first detailed CAD model is created, which will increase the quality of the first detailed simulation models and reduce the time to market. Moreover, early what-if studies can be performed to balance and optimize possibly conflicting performance attributes (safety, NVH, dynamics, durability ...) at an increased feasibility and at reduced costs [1].

In an effort to shorten development times, concept modeling CAx-methods play an important role in automotive industry. In so-called upfront CAE processes, concept methods are introduced earlier in the functional car development phase. The goal is to realize as early as possible a full vehicle concept, satisfying all functional performance requirements, such as for vibration and acoustics comfort. Very high costs for late concept changes and costly investigations on hardware prototypes are therefore avoided.

The modeling process comprises the assessment of different concept variations from the very early design stages up to detailed construction and optimization in the pre-series and series phases.

Using concept modeling applications, the designer can evaluate a large number of solutions and define, in a relative short time, the most suitable structure capable of meeting the structural targets within the defined design space.

In the early design phase concept methods are very powerful for suitability and feasibility studies, however they are characterized by a lack of accuracy and robustness, a main drawback that relegates them to a more qualitative rather than quantitative design/research techniques.

The aim of this research activity is therefore to provide a more powerful car body concept modeling method, seeking for higher accuracy and robustness, reducing development time and costs.

The most critical area of the concept modeling approach is clearly the characterization of the joints, a new joint modeling solution has been proposed introducing the so called “FEM hybrid structures”, whereby one-dimensional FE elements are coupled with three-dimensional joint structures and morphing techniques are applied to the three-dimensional parts in order to perform a full-body geometrical optimization process (see paragraph 4.1).

The implementation of hybrid structures in the concept model is a complex task, in particular the definition of congruency equations for the rigorous connections of the dissimilar elements (1D-3D) is a major engineering challenge and represents nevertheless the ultimate target of this Ph.D dissertation.

1.2 Introduction to the vehicle concept modeling

Concept modeling FEM design processes are well known modeling techniques and widely applied in the early design phase of any complex structure that must fulfill a set of global multi-disciplinary and high-performance structural requirements.

The key idea behind the concept modeling approach is to create a simplified car body model with a certain degree of parameterization, keeping in mind that it should be “as coarse as possible, as detailed as necessary”. The simplification of the model is normally realized by reducing the number of nodes and introducing geometrically simplified elements (mono-dimensional FE elements), while the parameterization can be realized in different ways depending on the software in use (i.e. introducing specific parameterized elements, using external solver, etc…). The reduced number of nodes assures a shorter calculation time while the parameterization defines the optimization variables.

Besides the concept modeling commercial software, like “SFE concept” or dedicated modules integrated in the CAE-driven development software (e.g. CATIA), the mainstream concept modelling approach is based on the combination of mono-dimensional thin walled parameterized beams and two-dimensional shell elements, defining the three dimensional structures. The car body structure is virtually divided in beam-like parts, carrying the loads, and panels. The structural parts are modeled using mono-dimensional beam-like elements with assigned bi-dimensional cross section properties, while the panels are modeled using shell-like elements, whereby a coarsening process is used to reduce the mesh discretization to the level of the mono-dimensional beam-like elements.

The car body concept modeling, based on combination of mono and bi-dimensional elements, is a well-established design process, so called "beams and shells” concept model and it is used for early concept phase car body structural optimization with a special focus on the NVH performance [2] [3] [4] [5].

The idea behind the “beam and shell” concept modeling is to transform as much as possible geometrical information of the FE model into properties information in order to create a model fast to calculate and easy to parameterize, that means easy to optimize.

An FE-model for the early concept phase has different requirements compared to one for the series development. Typically detailed CAD-geometry informations are not necessary and even not available. In this context of lacking geometric information and of demanding for quick answers in a short time, the simulation with so-called “beam and shell” FE models has proven to be a very effective process. The purpose of the investigations based on the “beam and shell” model is to evaluate the potential of different structural geometrical and topological

solutions in order to achieve premium NVH performance with minimum weight and construction space, while matching a complete set of vehicle customer relevant functional requirements, also including basic requirements for ride, handling and crash.

A fine FE model of a vehicle body usually consists mainly of 2D shell elements. The use of shell elements is appropriate where one dimension is small compared the other two dimensions, these elements are characterized by the fact that only two dimensions are modeled by nodes, while the third dimension (i.e. the thickness) is specified as a property. Considering that a body structure consists mainly of joined metal parts, a fine FE shells model is a perfect solution for a detailed representation, however not really suitable for topological optimizations in the early design phase.

In the early vehicle concept phase, where clear structural performance targets are set (dynamic stiffness, static stiffness, crash performance, acoustic and vibration comfort performance, etc.), but geometrical information are limited (wheel base, car width), the “beam and shell” model proves to be effective for global car body structural investigations and optimizations. An example of a BMW “Body in White” (BiW) concept model with arbitrary beam cross sections is shown in figure 1.

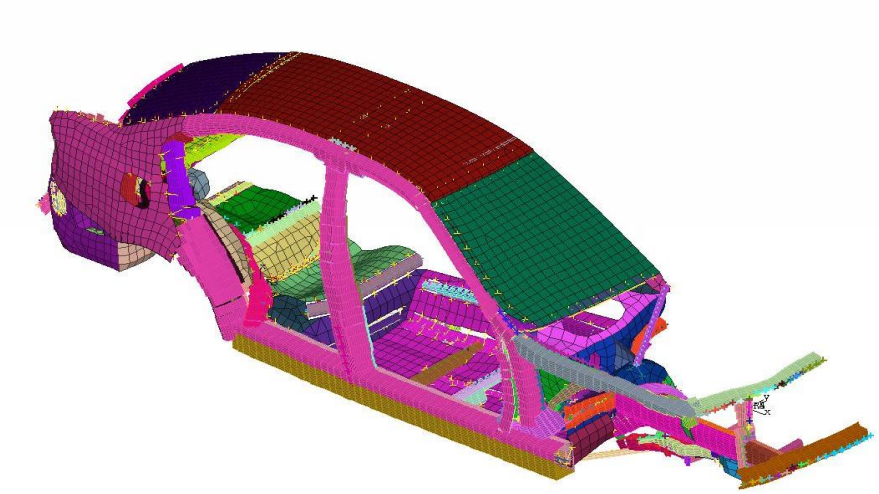

Figure 1 BiW concept model with arbitrary beam cross sections

1.3 Concept modeling “state of the art”

Design processes, especially in the concept design phase, are part of the core know-how of any engineering company, hence defining the “prior art”, defining the “state of the art” while positioning the BMW “beam and shell” concept model, is not an easy task. A meaningful way to place the BMW modeling approach with respect of the prior art is to evaluate individually the single technical features of the model itself.

The key technical features characterizing a concept model can be summarized as follows:

- Type of mono-dimensional thin walled beam model
- Type and number of variables
- Type of constraints
- Type of load cases
- Type of optimization strategy
- Type of connections between beam and bi-panel elements
- Type of joint modeling

Considering that:

- The “beam and shell” model is based on arbitrary beam cross section mono-dimensional beams with 7DOF (for more information, see paragraph 1.5), and that these are the most advanced mono-dimensional FEM beams available in commercial software (in literature, models with higher number of DOF are available, however they are defined just for a restricted type of cross sections and still under validation);
- The “beam and shell” model has more than 1500 variables describing completely the geometry of the BiW, (large scale optimization problem), normally in the automotive applications a maximum of 300 variables are used;
- Constraints and load cases of the “beam and shell” model are the same applied in the development of the static and dynamic BiW structural performance during the final phase of design at BMW;
- The optimization strategy of the “beam and shell” model (see description in chapter 2) has been recently developed and tested within the VECOM project, providing best results in concept modeling applications;

- The connections between beam and bi-dimensional panel elements are rigid standard connections and specifically designed to emulate with a minimum error the structural behavior of the welding spots.

It is possible to state that the “beam and shell” model represents the “state of the art” in the field of concept modeling for static and dynamic investigations. The solution to the problem posed, lack of accuracy and robustness, has to be found in the definition of the joint modeling approach, clearly playing a dominant role in this context.
A general description and a critical review of the car body design and optimization process is presented in the upcoming paragraphs. The focus is on the latest joint modeling solutions, introduced to increase the robustness and the accuracy of the modeling process (see chapter 3).

1.4 Concept model construction

The main idea behind the creation of a “beam and shell” model (BS model), is to describe the geometry as much as possible through properties of elements instead of the actual geometrical coordinates of the nodes of the elements. Using full shell-FE models only plate thicknesses are available for optimization, whereby the use of mono-dimensional beam elements allows a parametric description of the complete beam cross section, using beam width, height and the respective wall thicknesses.

To start the creation of the BS model, see figure 2, the designer selects a suitable starting model ranging from just sketches, a full CAD model, a predecessor fine FE model, a predecessor BS model or a mixture thereof. Basically it depends on whether a brand new car concept is being developed or whether it is more an evolutionary development of a predecessor.

The geometry of the selected starting model is then first subdivided into regions for beam modeling, consisting of the main load carrying structure of the body, and the shell-like rest of the structure, consisting of the body panels. All the beams are modeled using mono-dimensional elements with assigned bi-dimensional cross section properties. The rest of the body is kept as shells elements, where a coarsening process is used to reduce the mesh discretization to the level of the mono-dimensional beam elements. The beam and shell elements are then coupled together using an in-house rigid-connections coupling scheme forming the final FE concept model.

When modeling from scratch, i.e. based on a limited set of dimensions and sketches, the mono-dimensional beam elements have to be generated in dedicated standard CAE pre-processors. More often however the modeling starts from existing shell element models, whereby the mono-dimensional beam elements and their section properties can be largely automatically generated by cutting the shell elements along the beam-like structure (an in-house tool has been developed for this process but equivalent commercial tools are also available). Based on the cut section geometry, the tool generates the actual nodes and elements across the centers of gravity of the section cuts of the beam-like structure, evaluates the section properties and the actual geometry of the beam cross-section in term of line segments. If necessary this line segment geometry information can then be imported in dedicated cross section editors for further simplification and modification. Once all the beam cross sections have been defined, the generated beam properties can be assigned by the user to the beam elements in the FE preprocessor.

Using the FEM standard property definition, the actual geometry of the cross section is no longer available and therefore not accessible during the optimization process. In an iterative optimization sequence these geometrical properties are therefore converted using an in-house tool to equivalent properties, in terms of cross sectional area and moments of inertia that can be edited.

The FEM solver beam library includes a series of basic geometric shapes such as e.g. rectangular, U-profile, L-profile, I-profile, etc. In general closed sections will be modeled with rectangular-type sections and open sections with U-profile type sections. When using open sections the important cross section 'warping' effects will be taken into account. The property entries for the FEM solver standard sections consist of dimensions describing the standard basic cross section geometry, such as width, height and wall thicknesses. These dimensions can be directly addressed as design variables in the optimization sequence.

In recent years however, a more sophisticated approach to model beam cross sections has been introduced, the so called "Arbitrary Beam Cross Sections" (ABCS) method, allowing an exact geometric definition of the beam cross section. Two different geometry descriptions are available. For the so-called GS-sections, the cross section geometry is described by the area defined of an outer-loop and a series of inner-loops.

The second definition is the so-called center-line description, suitable for thin-walled structures, whereby a series of line segments describes the medial line of the cross-section and wall thicknesses can be assigned on the level of each line segment. The bounding box height and width of these ABCS cross sections, as well as the wall thickness for the center line sections, are available as design variables for the optimization sequence. A more detailed description of the method is provided in section 3.

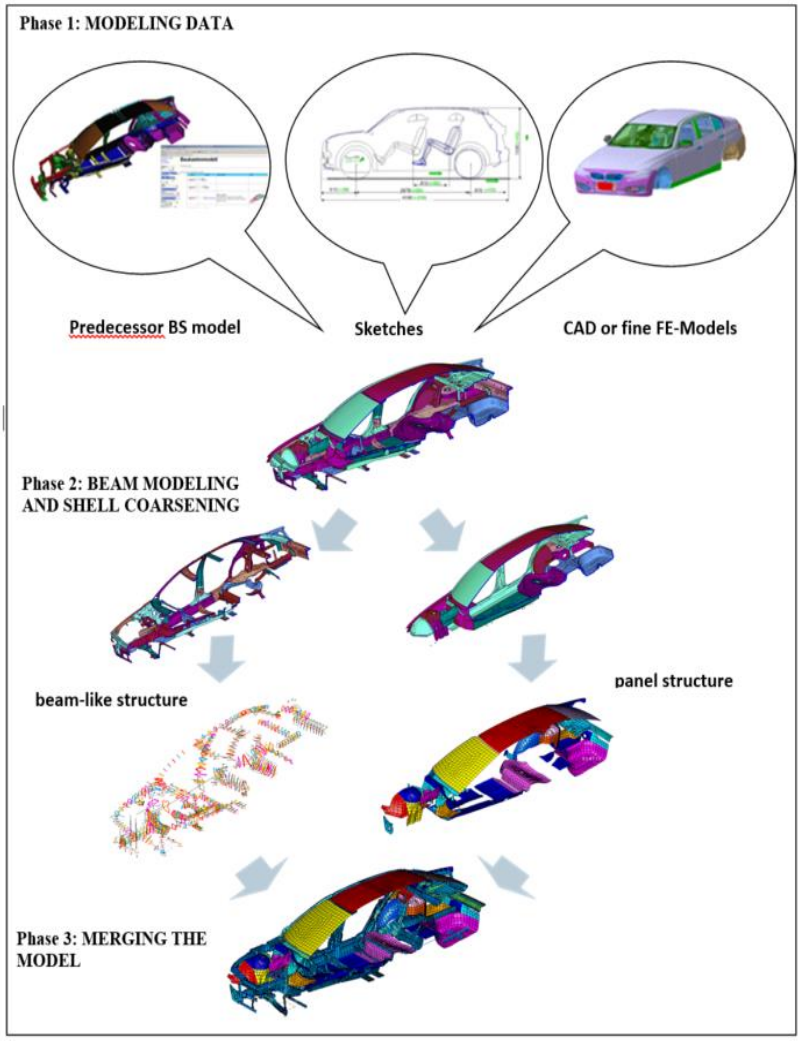

Figure 2 Workflow for the creation of beams and shells FE concept models

A very important modeling aspect is the connection of the beams in the different car body structure joints, where three or more beams are to be connected. Empirical rules have been defined at BMW to model these joints with a combination of open- and closed beam sections based on the judgment of the actual 3D-geometry

of the joints and the presence of internal lateral or longitudinal stiffening plates inside the joint structure.

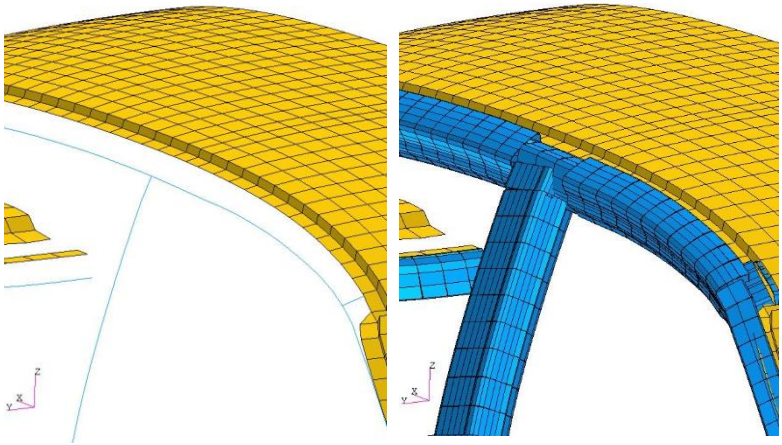

Figure 3 Joint between upper B-pillar, upper side frame and middle roof cross beam

In figure 3, the modeling of the joint between upper B-pillar, the upper side frame beam and the middle cross roof beam is shown. Especially the joints connecting the A-, B-, C-pillars to the rest of the structure play an important role in global car body stiffness and should be modeled with care.

The remaining panel structure of the car body structure is meshed with shell elements with a mesh discretization equal to the size of the beam elements. The beam and shell structure is then merged together and connected through rigid connectors using an in-house connection scheme. To finalize the BS concept model a series of special points are set using an in-house numbering scheme identifying the relevant load, constraint and response positions, enabling standardized automatic definition of the different load cases. The beam and shell elements of the car body are then subdivided in predefined logical groups according to the different car body parts. These logical groups can be addressed for global constraints settings for the optimization sequence (see next section), as well as for added mass distribution for setting up trimmed body FE concept models. A set of standardized trace lines is defined along the beam-like structure of the body, enabling automatic post-processing and visualization of the results. The model is then finally subjected to standard calculation runs, including modal analysis and global static bending and torsion load case, for a model quality check [4] [5].

1.5 ABCS beams

In this section the advantages of the implementation of the arbitrary beam cross sections applied on the BMW “beam and shell” models, are discussed.

In general, in commercial FEM software three different types of mono-dimensional beam models are available for concept modeling applications:

- 1D beam model with equivalent cross section: no geometrical information included.
- 1D beam model with equivalent standard cross section selected from a library (C, T, circular shape etc..).
- 1D beam with arbitrary beam cross section, ABCS.

The big drawback of using the equivalent cross sections or the limited set of the equivalent standard cross sections from the beam library is the total loss of the actual cross section geometrical information. After the optimization only statements on the level of cross sectional geometric properties can be done. The link to the actual optimized cross section geometry is no longer available, as shown in figure 4, [2] [4].

The use of ABCS beams allows for geometrically exact description of any real beam cross sections, described through property cards.

The ABC-sections can be defined through a “general” and through a “center line” section description. For both descriptions the bounding box width and height can be defined as design variables in order to realize a 2D scaling of the real cross section. The center line description is particularly suitable for thin-walled cross sections. Using this description it is not only possible to allow for 2D bounding box scaling, but also the thicknesses of wall segments are available as design variables. The arbitrary cross section shown is an ABCS beam section of type center line. An additional advantage of the ABCS description is the possibility to explicitly handle longitudinal internal stiffeners in the optimization sequence. In the standard section approach these stiffeners ‘disappear’ in the ‘equivalent’ section properties and are consequently not directly accessible through a design variable in the optimization sequence.

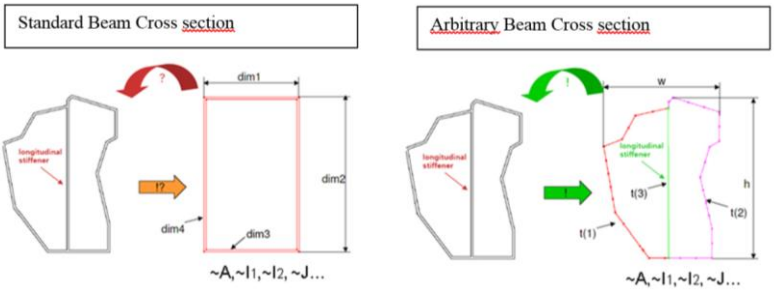

Figure 4 Cross section of a rocker panel modeled using a standard section (left) and an arbitrary cross section (right).

The benefits of running an optimization process with the ABCS beams compared to the standard sections of the beam library can therefore be summarized as follows:

- Direct optimization of the real cross section geometry: not only qualitative but also quantitative information is available to improve the body structure in terms of bounding box size and wall thicknesses.
- Description and optimization of sections with longitudinal stiffeners is only possible with ABCS beams .
- Higher acceptance of the results by the designers. The designer recognizes his beam construction.
- No conversion to equivalent standard cross section necessary The introduction of the ABCS beams provides considerably more flexibility for design changes in the different optimization cycles. The overall 2D scaling of the beam cross section bounding box in the optimization sequence can indeed still be seen as a limitation. However it is considered as an important step towards full parametric beam cross section modeling and optimization.

1.6 Multi-attribute optimization of the concept model

Once the complete concept model has been created, a set of 1500 FEM variables and a multi-objective optimization function are generated, the target of the optimization process is to minimize the weight, investigate potential construction space, while matching the global relevant customer requirements. A representation of the full optimization process, including the model build up phase, is displayed in figure 5, [5].

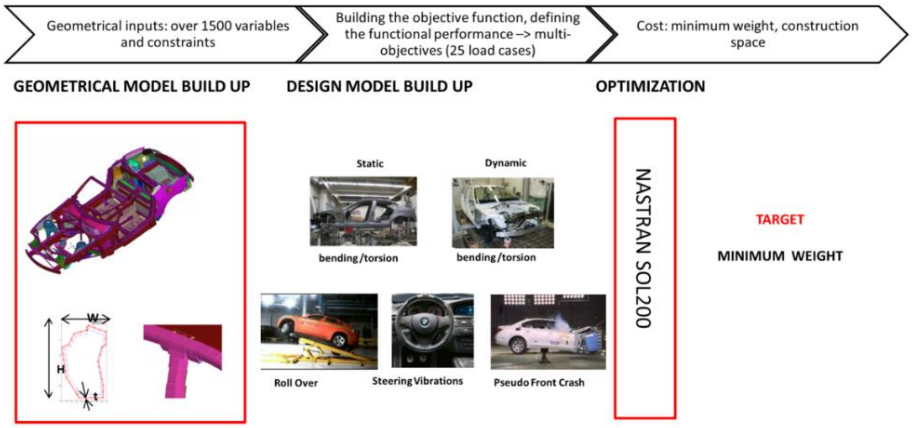

Figure 5 Representation of the optimization process including the model build-up phase

The optimization functions include 25 different load cases, each load case has a different weighting factor that can be weighted depending on the design requirements. The 25 load cases can be grouped in 5 main categories:

- Static stiffness
- Dynamic stiffness
- Roll over (linearized)
- Steering column vibration
- Pseudo front crash (linearized)

The aim of the investigations is to ensure premium NVH performances for the “Body in White” in different operational conditions. The most important study case is the dynamic stiffness one, however a multi objective approach has been developed in order to ensure, already in the concept phase, the achievement of all

the global structural performance, including crash, avoiding late and expensive design modifications.

1.6 Multi-model optimization

An interesting aspect of the beam and shell concept model is that can be easily applied nowadays for parallel multi-model optimizations. The always higher degree of standardisation of the body in white components required by the OEMs to keep low the manufacturing costs while assuring high-quality standards, drives the designers to implement a modular design approach. This approach leads to an always higher number of components shared between different car bodies of the same line-up (and sometimes even of crossed line-up). In figure 6 an example of the possible common components shared among three different car bodies of the same line-up is shown. Once the concept models of the three car bodies are created, the same set of optimization parameters can be assigned to the shared components (in orange) of the three different car bodies. Different optimization targets for each vehicle can be defined, according to the different structural requirements, and finally a single optimization function for the unique set of design variables of the shared components can be defined. Finally a parallel FEM calculation of the bodies can be executed. The great advantage of a multi-model concept optimization is that a set of common shared parts can be optimized at the same time for the different structural requirements of several vehicles.

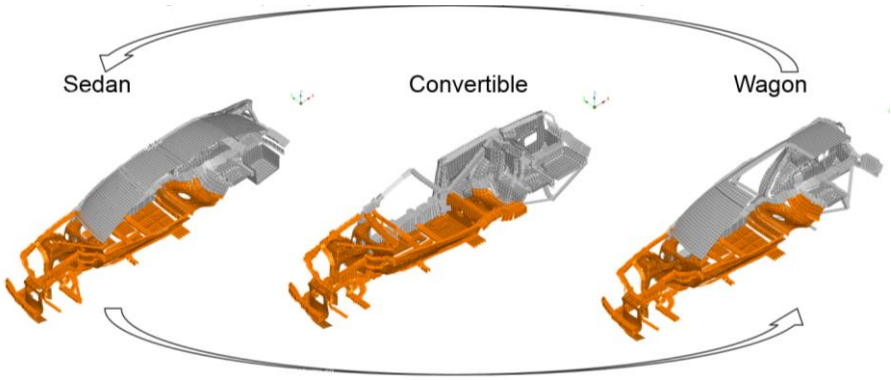

Figure 6 Example of shared parts to be optimized in a multi-model optimization

2 OPTMIZATION STRATEGY

In this section, a brief overview of the strengths and weaknesses of genetic and gradient-based algorithms, in the context of optimization problems whereby each function evaluation is relatively expensive, is given. The focus is on problems in which the number of design variables is significantly greater than the number of objectives and constraints, more details on the optimization strategy and penalty method implemented in the "beam and shell" model are also given.

2.1 Optimization strategies: general overview

In figure 7 a scheme gives a general overview of the possible optimzation strategies applicable for BiW optimization sequences.

In gradient based strategies, the cost of the optimization can be considered roughly proportional to the number of design variables. Rapid convergence is the primary advantage of a gradient-based method. Clearly, proper exploitation of gradient information can significantly enhance the speed of convergence in comparison with a method that does not compute gradients. Another feature of gradient-based methods is that they provide a clear convergence criterion. If the gradient is reduced by many orders of magnitude, one can be confident that at least a local optimum has been reached.

One of the key disadvantages of gradient-based methods is the "development" cost. Whether the linearization is performed by hand or using automatic differentiation, with a complex code this can be time-consuming. Another potential weakness of gradient-based methods is that they are relatively intolerant of difficulties such as noisy objective function spaces, inaccurate gradients, categorical variables, and topology optimization. Another oft-mentioned disadvantage of gradient-based methods is that they find a local rather than a global optimum.

However, in many engineering design contexts this is unlikely to be an issue, since the highly constrained nature of the design problem inhibits multimodality. The key disadvantages of gradient-based methods are precisely the strengths of genetic algorithms. First, genetic algorithms treat the function evaluation as a “black box”. Consequently, development cost is minimal. Second, they are tolerant of noise in the objective function and have no difficulty with categorical variables or topology changes. Furthermore, in principle, genetic algorithms find a global optimum. The key disadvantage associated with genetic algorithms is that they can converge very slowly, especially near an optimum. A second weakness is that determining a termination criterion is not straightforward.

It is not yet well understood how well either a gradient-based or a genetic algorithm can deal with such design problems. Although a genetic algorithm can proceed in principle, insufficiently converged solutions can produce misleading results that can lead the genetic algorithm into nonoptimal areas of the design space.

The above strengths and weaknesses must be considered in choosing an optimization algorithm for a specific problem class. A key tradeoff is between the relatively high development cost of the gradient-based method using an adjoint formulation and the relatively high computational cost of the genetic algorithm. The more frequently the algorithm is to be used, the more beneficial the gradient-based algorithm becomes. Clearly, a quantitative assessment of the computational cost of the two algorithms is needed to make an intelligent choice for a given class of problems [6][7][8][9][10].

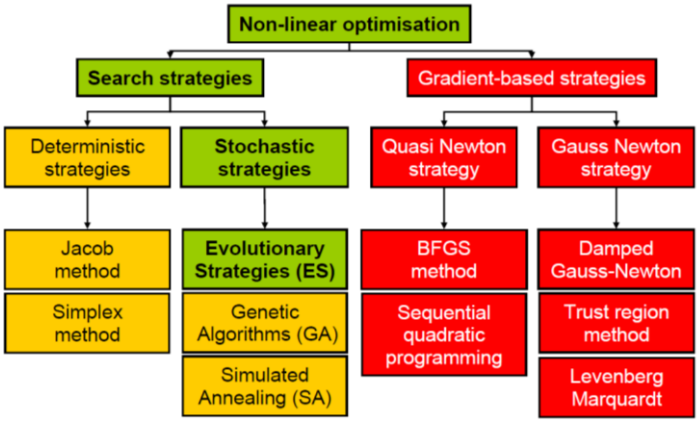

Figure 7 Optimization Strategies

2.2 Optimization strategy of the concept model

The “beam and shell” multi-disciplinary vehicle optimization process is built around a gradient based solver.
A gradient based solver has been preferred over a genetic algorithm because of the rapid convergence, the drawback of finding just local minima is partially counter-measured launching the gradient based solver optimization starting from different initial design configurations, up to ten times, increasing consistently the chances of approaching a global minima.
The setup of the optimization model includes the identification of the design variables, setting-up the design constraints and the optimization cost function. For the optimization sequence of the car body a series of relevant load cases are taken into account for optimal full vehicle NVH as well as ride and handling performance. These cases include a series of global static bending and torsion load cases, car body eigen-modes, frequency response functions at customer relevant locations and local static stiffness at chassis connection points. These levels of static stiffness will indeed directly influence the accuracy of the steering response and the overall driving experience, as the body is acting as a spring between the two axes during driving maneuvers. On top of that a pseudo crash load case is included, in order to take into account minimal crash requirements for the car body in an approximate way as well. For all these load cases specific targets are set for the car body, based on detailed analysis of customer relevant functional performance requirements for the full vehicle. The objective of the optimization is to find an ‘optimal’ car body structure with minimal weight, satisfying the different load case targets and constraints within the available construction space of the car body. For the complete study of a body structure up to 1500 design variables are taken into account while considering an equivalent number of constraint equations.
A tailored penalty method so called ß-Method (see paragraph 2.4) is also included in the objective function in order to increase the chance of getting optimization results into the feasible design area [2] [4].

2.3 Creating the optimization model

The setup of an optimization model of about 1500 variables is a challenging and important modeling phase, it includes the identification of the design variables, setting-up the design constraints and the optimization cost function and requires a high degree of automation. In this paragraph the automated approach developed for the “beam and shell” model is described [2].

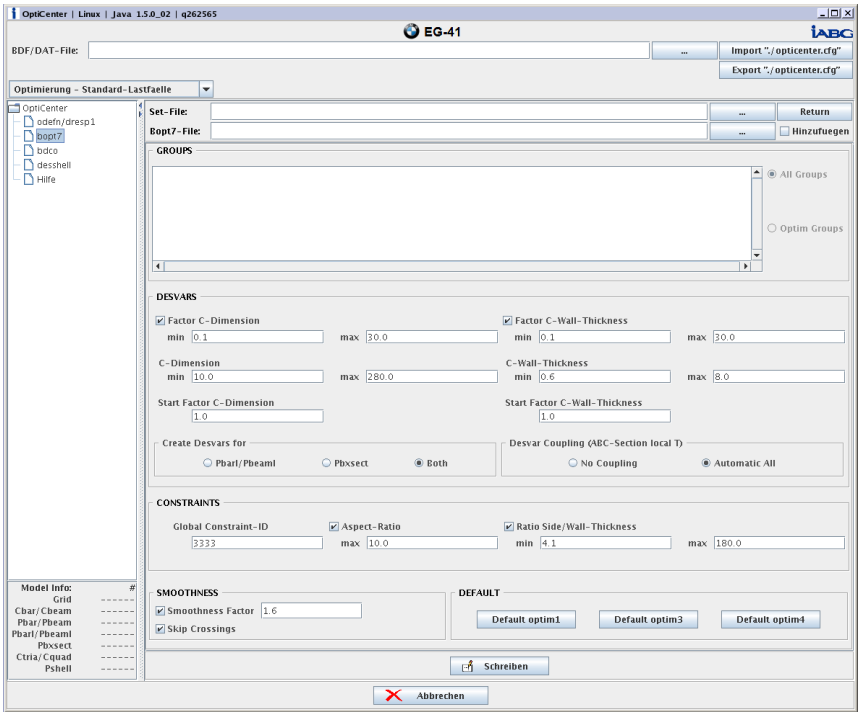

Figure 8 OptiCenter GUI for setting-up design variables and constraints

The objective of the optimization is to find an “optimal” car body structure with minimal weight, satisfying the different load case targets and constraints within the available construction space of the car body.

The available construction space of the car body is defined by setting the beam cross section geometrical parameters – height, width and wall thickness – as design variables with suitable min/max limits, based on full vehicle package and design, technological and manufacturing (e.g. minimal sheet metal thickness, width/height ratio of beam structures, etc.) constraints. For the complete study of a

body structure up to 1500 design variables are taken into account while considering an equivalent number of constraints equations.

To facilitate the definition of this large set of design variables and constraints an in-house tool so called OptiCenter, see figure 8, has been developed. Based on the imported FEM bulk data file of the concept model and the predefined logical groups the design variables are automatically identified and design limits are set based on predefined default settings or specific user input. The corresponding FEM cards are created and exported into the input deck.

Using the same tool the different load cases to be considered can be selected and necessary target values can be specified by the user as shown in figure 9. For the global dynamic car body stiffness up to four eigen-modes can be targeted during the optimization. The user provides the target frequency level, the mode shape type (i.e. 1. bending, 1. torsion, 2. bending, etc.) and the mode number necessary for the mode tracking during the optimization iterations. Furthermore a minimal frequency difference between two modes can be targeted, e.g. 3 Hz between first global modes.

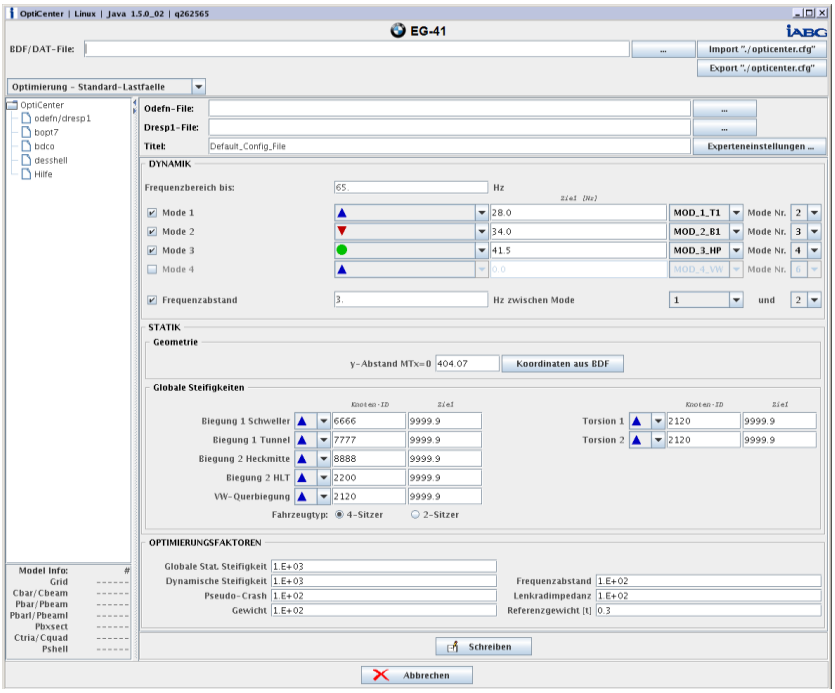

Figure 9 OptiCenter GUI for dynamic and static load case specification and targeting

The identification of the targeted modes are evaluated in a nominal run, the so-called check-run, where all load cases are evaluated for the starting configuration of the concept model.

Regarding the static stiffness, a series of standardized equivalent static bending, torsion and lateral stiffness load cases have been defined for the car body and handled in the multi-load case optimization sequences. Target values, as well as the location where the static stiffness values have to be evaluated, identified in the nominal check run, are specified by the user. The target static stiffness values are converted to static deformation levels in the specified locations.

Next to these main load cases, targeting overall optimal car body stiffness, a series of pseudo frontal and rollover crash load cases are taken into account, ensuring minimal crash requirements for the car body. The frontal crash load case is set-up as an inertial relief calculation, whereby the car body is deformed by the inertial forces induced by the crash impact forces. These pseudo crash and rollover load cases are targeted by specifying maximum allowable strain values in the beam structure of the green house of the car body.

More specific vibration comfort load cases can be specified as well in terms of frequency response monitoring. Steering wheel vibration levels are for example monitored in the relevant frequency range of the stationary regime of the engine.

2.4 The penalty method: ß-method

In the gradient based optimization sequence constraints are satisfied first, before minimizing the objective function. In the beta-method, the monitoring of the different load case targets is formulated as a constraint and introduced into the objective function through a newly introduced design variable (β), measuring the constraint violation.

These design variables so-called beta-values are combined with the car body weight into the objective function, whereby the relative importance of all load cases can be balanced in the optimization cost function by specifying relative weighting factors.

The above mentioned constraints are formulated in such a way that minimizing the beta-value implies reaching the specified target values. In the equation (1) the constraint equation is shown for targeting the eigen-frequency of a tracked mode as a minimal value [2].

$$2 + \frac{(f_{target} \cdot 2\pi)^2 - \lambda_{1st}}{(f_{target} \cdot 2\pi)^2} - \beta \leq 1 \qquad (1)$$

The same procedure can be done also in case that a variable should be below a certain maximum value or should match an exact target.

When the beta-method is used, a limit curve (f_{target}) is defined first, which is used for the normalization of the frequency response (λ_{1st}). With the help of the additionally introduced design variable β, whose starting value is usually one, the constraints are defined, the design objective becomes a function of the design variable β and a minimization or maximization of objective function can only be achieved through a minimization of maximization of β value. An important point is that introducing the beta-method several subcases can be optimized at the same time.

Without the beta-method, once the constraints have been violated the gradient-based solver would stop before minimizing the objective function, in order to prevent this situation, the constraints are "relaxed" through the additional variable beta and the objective function is minimized/maximized in function of the beta values, avoiding the termination the optimization sequence, reaching the target values.

The beta-method optimization sequence is based on a gradient based optimizer, this means that the optimized solution is found step-by-step in the direction of the steepest descent, identified by evaluating the sensitivities of all responses with respect to all design variables. A common problem with this type of optimizers is the convergence to local minima. No guarantee can be given on whether a global optimum has been found. A common procedure is therefore to re-start the optimization sequence from different initial configurations, in an effort to explore the full design space and therefore increase the probability to find a more global optimum. These different initial configurations can either be specified by the user or can also be generated randomly by perturbation of the design variables from the nominal design within the given limits.

2.5 Post-processing of the results

The gradient based optimization sequence for these coarse “beam and shell” FE concept models, handling well over 1500 design variables, generates a large amount of result data in the form of binary (op2) and ASCII files. Dedicated in-house post-processing tools have been developed in order to interpret these data in a comprehensive and standardized way.

Key-results are automatically extracted and presented in tables, graphs and contour plots in a dedicated intranet, allowing for quick reporting and results comparison when studying different car body concepts. Figure 10 shows the optimization history of the first bending (green line) and torsion (red line) mode versus their target value. Similar plots are generated for all static load cases, as well as, for the evolution of the car body weight to be minimized.

Three-dimensional contour plots of the full model are also generated with extensive information on the change in construction space, i.e. change of beam cross section width and height, and the change of beam cross section wall thicknesses. Figure 12 shows an example of a contour plot, depicting the change of the outer dimensions of the different beam elements. Such contour plots give a good overview on the areas of car body structure where constructive measures preferably have to be taken in order to achieve the set targets in an optimal way [2].

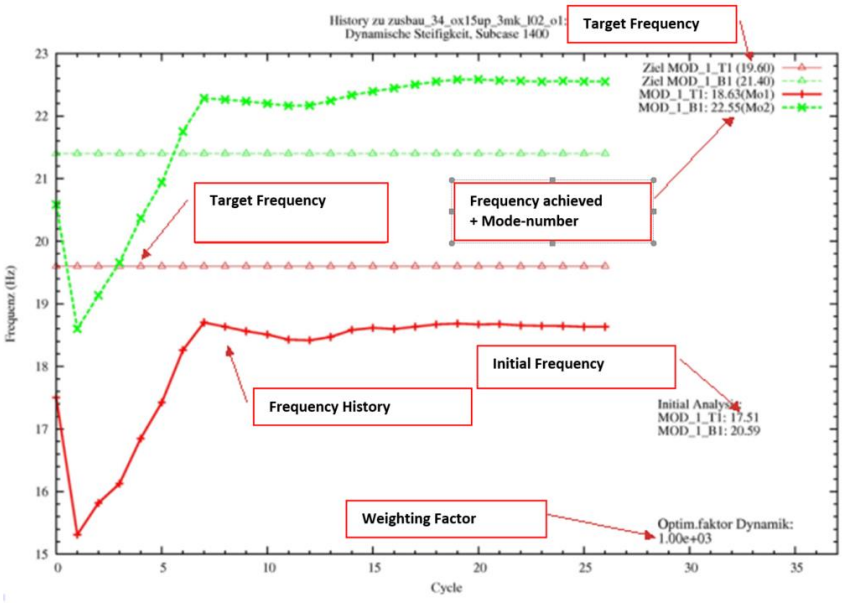

Figure 10 Optimization history of the first bending and torsion eigen-frequency.

2.6 Application case

In order to provide the reader with a better overview on concept modeling applications, a practical example of how the beams and shells concept modeling process has been recently used at BMW during the early concept development phase of new car projects is presented. The following type of design questions were to be analyzed:

- What are the structural modifications for a station wagon car body needed to fulfill significantly increased functional static and dynamic stiffness targets, while obeying different limitations concerning construction space?
- Can the proposed structural modifications be realized in the current design or is a new structural topology needed?

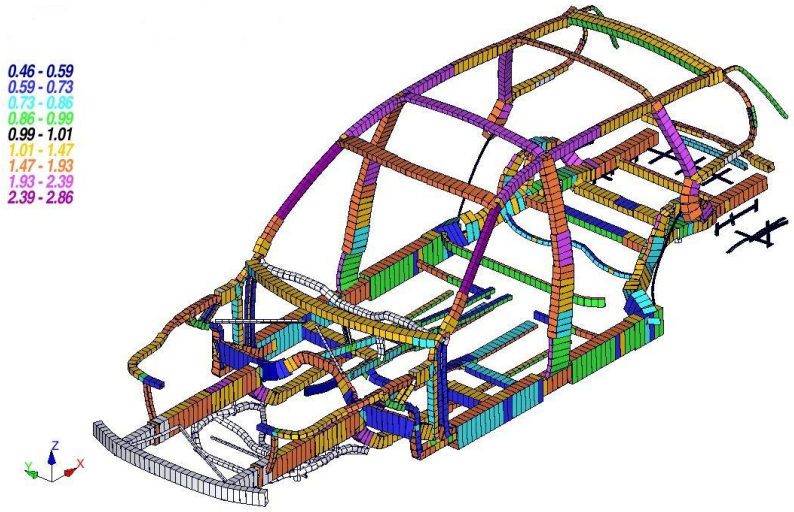

Figure 11 Change in wall thicknesses after an optimization of a station wagon car body structure with limited construction space

In figure 11 the optimized carrier structure of the reference middle class station wagon is shown with the optimization restriction that the existing construction space should not be exceeded. The colors show the scaling of the wall thickness with respect to the initial values. In this optimization run, the targeted dynamic stiffness could not be reached, even though wall thicknesses have been increased to up to 300 percent of the original values in some regions. Further increasing wall thicknesses clearly results more in an increase of mass than an

increase in car body stiffness, leading to a loss of dynamic stiffness and lower global eigen-frequency levels. Through the use of the earlier described beta-method, the optimization continued converging to the best-compromise solution while residing in an infeasible design region, not completely fulfilling the eigen-frequency target constraints.

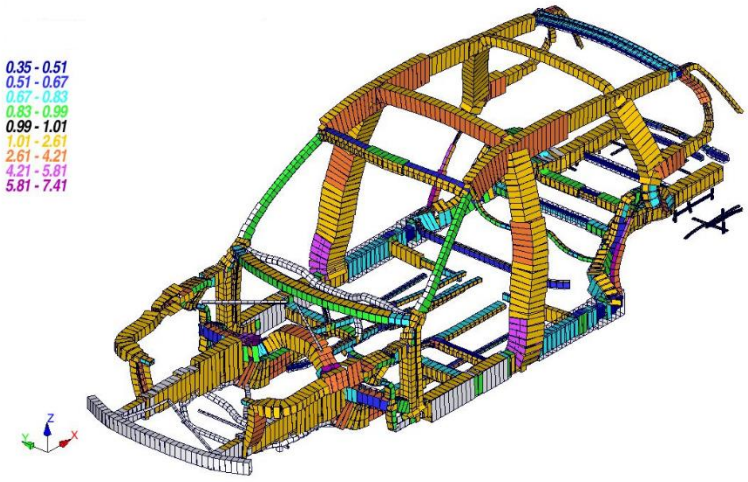

Figure 12 Change in construction space after an optimization of a station wagon car body structure without limitations for the construction space.

The scale reported in figure 12 is related to the relative change in construction space, i.e. the outer dimensions of the carrier structure after an optimization process where an almost unlimited construction space scaling is allowed. Special restrictions are set for the longitudinal front and rear carrier that are not allowed to shrink because of crash requirements and for the upper A-pillar, which is not allowed to increase due to design reasons.

With those boundary conditions, a significant increase of about 200 up to 700 percent in some areas of the car body structure can be observed. Especially for the roof carriers and the B-pillar the needed construction space increases enormously. The resulting extremely large carrier cross sections are not acceptable for package, design and ergonomic reasons. Further optimization runs with more realistic restrictions on the outer carrier dimensions have lead again to best-compromise results without reaching the dynamic eigen-frequency target values.

From these examinations the conclusion was drawn, that the car body structure of this middle class station wagon is not very well suited as base for the new considerably increased dynamic stiffness targets. The increased functional requirements clearly call for an alternative carrier topology [2].

3 CRITICAL REVIEW OF THE CONCEPT MODEL

In this chapter a critical review of the "beam and shell" model based on "strength and weaknesses" analysis supported by simulation data is presented. The focus is on the most critical part of the BiW concept model: the joints. The actual joint modeling approach, the "state of the art" of the joint modeling and a new solution are also presented.

3.1 Strengths and weaknesses analysis

The "beam and shell" model for the early design phase of the body in white presents, according to the opinion of the author and of a group of experienced engineers in the field of concept modeling (a survey has been conducted among seven experienced engineers), the following strengths and weaknesses:

Strengths:

- Short calculation and optimization time.
- Multi-model optimization: parallel optimization of common parts, shared in different vehicles with different structural targets.
- High degree of geometrical details in the concept phase: the full geometry of the cross-sections is maintained (ABCS).

Weaknesses:

- Low modeling accuracy due to inconsistent joint modeling approach.
- Long modelling time.
- Density correction factor needed in order to take into account the loss of mass due to the lack of minor components (e.g. door hinges, plastic sub-frames etc..).
- Not yet suitable for composite materials.

3.2 Modeling error

The beam and shell model is a useful design tool in the early car design phase for feasibility studies, the model has been developed in house for years, parallel to a wide set of dedicated pre and post processing tools. A detailed list of rules and design guide lines are also provided and made available on-line internally. Despite those efforts, the modeling error is relatively high and the modeling process has a low level of repeatability.

It is well known among modeling experts that the most critical part of the "beam and shell" model design process is the characterization of the joints, the global static and dynamic stiffness of the car body depends mostly on the right modeling of them. A set of tests have been done in order to identify all the possible source of error of the model, taking into account several modeling aspects, the results confirmed the dominant role played by the modeling of the joints. Minor changes on the modeling of the joints (within the BMW standards and guide lines) could increase noticeably the modeling error, up to the double of the expected values.

In the graph of figure 13, the different deformations lines of the full body of a BMW E90 are described. The red lines describe the deformation lines of the reference model (fine FE model) under certain loads (load related information are confidential) versus six different concept models realized by six different designers following the internal standard and modeling guidelines. The six concept models reported in figure 13 differs from each other mainly for the modeling of the joints, however the resulting models show quite a significant difference between each other (a quantitative comparison is not provided due to confidentiality). In other words each designer, deriving a concept joint form the reference fine model, has to "interpret" each joint thus resulting in a non-consistent quality of the concept model, strongly dependent on the experience of the designer.

Additionally the quality of the current beam and shell concept model has been assessed comparing a fine FE model of a BMW E90 (reference model) with a "beam and shell" model directly derived from the same fine model. The two models have been investigated under same load cases and the result cross-checked with the measured data of an E90 BiW available from the BMW measurement center, see figure 14.

More in detail, the comparison was based on two different static load cases, bending and torsion, the results from the modal analysis have been also compared, first bending and first torsion eigen-modes.

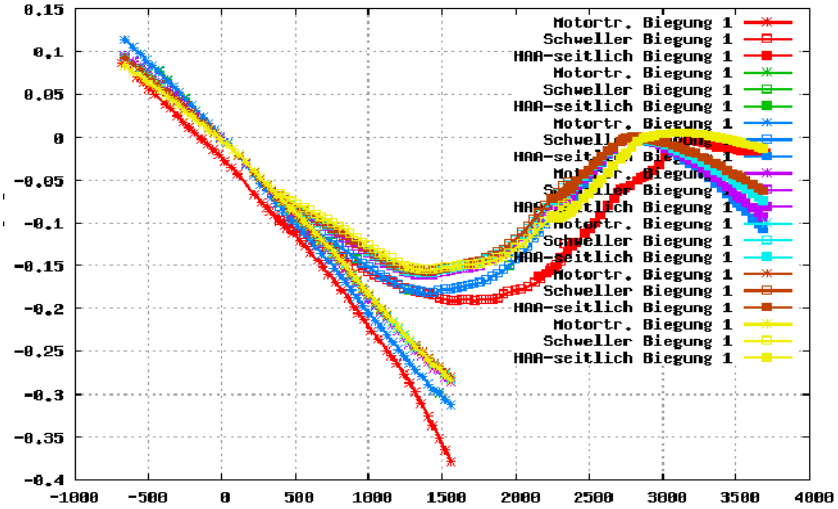

Figure 13 Deformation lines of different E90 BiW models

Figure 14 Models and data analyzed for the evaluation of the quality of the "beam and shell" model

From these two load cases, 10 different values describing the static stiffness of the BiW are calculated and compared (e.g. global bending stiffness, front local stiffness green house). For a full understanding and description of the deformation status of the model also five trace lines have been defined and compared. The total mass, the position of the center of gravity and principal axes of inertia have been also compared.

The result of assessment can be summarized as follow:

- The total mass, principal axis of inertia and the center of gravity of the concept model differs from the reference model of ~1%.
- The global static stiffness in bending case is forecasted within an error of ~5%.
- The global static stiffness in torsion case is forecasted within an error of ~8%.
- The local stiffness is forecasted with an error depending of the different cases, max: 30%.
- The error of the dynamic stiffness is evaluated through a MAC matrix and is about 5%.

Additional modeling aspects that are worth to mention are related to the welding spots and flanges. The effect of the distribution of the welding spots is unfortunately not taken into account in the concept model, however considering that the concept model is in general quite diverse from the final production model and that it is used mainly for qualitative studies, this is not a critical aspect.

Regarding the flanges, the cross section of the mono-dimensional beam of the concept model are modeled without flanges, reducing in this way the moments of inertia of the sections, this it is done in order to compensate the augmented stiffness due to the fact that the mono-dimensional beam are completely closed along the longitudinal axes, because, as already mentioned, the welding spots are not modeled.

3.3 Joint modeling: actual situation

In order to provide a better understanding of the actual joint modeling approach used for the realization of the “beam and shell” model, in this paragraph a short description of the method, using practical examples, is provided.

Each joint of the concept model is modeled using a combination of mono-dimensional beams with open or closed profiles depending on the actual geometry and topology of the reference joint. For each type of joint, the designer has to decide, following the guidelines and the internal standard, which combination of profiles need to be used in order to characterize in the most accurate way the joint, taking also into account eventual reinforcement plates.

For instance in figure 15 and in figure 16 the guidelines for modeling two different joints connecting the B-pillar with the rocket panel are shown. The figure 15 indicates that in case the joint has three reinforcement plates, it needs to be modeled using beams element with closed cross sections in the three directions, while in figure 16, in case the joint has two reinforcement plates, it should be modeled using a combination of one beam with closed profiles and the other two with open profiles. All the geometrical parameters of the beams in red are parameterized and therefore can be optimized.

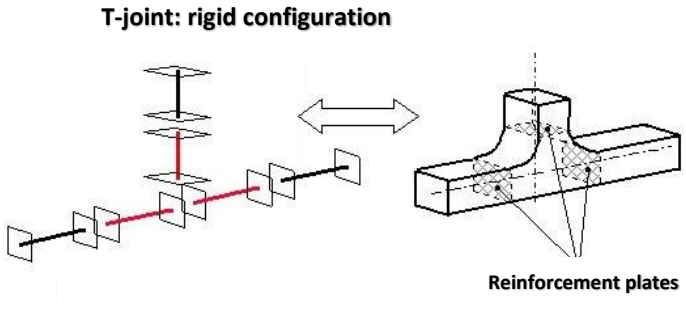

Figure 15 Example of modeling guideline for a joint modeling in the “beam and shell model” with three reinforcement plates

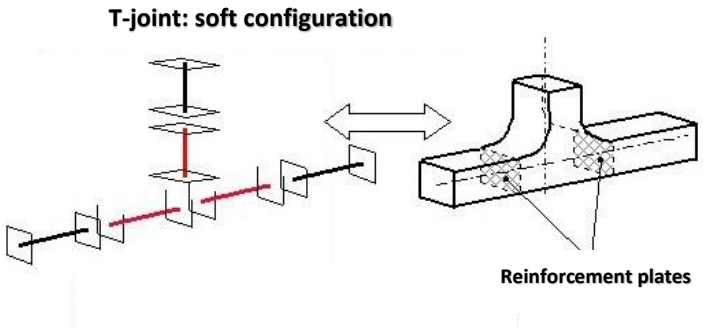

Figure 16 Example of modeling guideline for a joint modeling in the “beam and shell model” with two reinforcement plates

The main asset of the current modeling approach is the possibility of optimize the full body without losing completely the related geometrical information, however the price to pay is a lower accuracy, due to the “interpretation” of each joint that the designer as to perform.

In the following paragraphs a “state of the art” of the joint modeling and a new modeling approach combining a high calculation accuracy while keeping the geometrical optimization applied to joints and other complex structures is presented.

3.4 State of the art of the joint modeling

In order to find a solution for a more robust joint modelling approach, the "state of the art" of the joint modeling has been defined.

In literature fifteen different solutions have been found, selected and evaluated according to the following criteria [11][12][13][14]:

- Modeling time
- Calculation time (SOL200)
- Stress calculation (possible yes/not)
- Geometrical information
- Repeatability
- Accuracy
- Need of external solver (for optimization)
- Innovation degree
- Optimization information (geometrical information available after optimization)

All the concept joint modeling approaches found in literature are more or less sophisticated implementation of:

- super-elements
- spring-joint representations

The super-elements and spring-joints models have two main advantages: accuracy and repeatability.

The super-elements have been also tested on the "beam and shell" model confirming the expected accuracy.

However they have two main drawbacks: total loss of geometrical information during the modeling phase and no chance to perform stress calculation.

Due to the above mentioned drawbacks, both solutions, the super-elements and the spring-joint modelling, have been judged "not suitable" to be implemented in the beam and shell model.

A new joint modelling approach based on hybrid structures, whereby mono-dimensional beam-like elements are coupled with three-dimensional detailed joint structures, providing accuracy and repeatability while keeping the needed geometrical information and the possibility of calculating the stress of the structures

has been implemented, a detailed description of this solution is given in the upcoming paragraph.

A summary of the evaluation of the modeling solutions including the new proposed solution is shown in figure 17.

All the joint modeling approaches have been assessed referring to the actual BMW method based on a combination of beams with open and closed arbitrary cross sections. At the BMW method has been assigned the value 0 for each criteria assuming it as the reference, each criteria of each model has been evaluated following the scale below.

SCALE

2	This modeling method has a clear advantage regarding this aspect
1	This modeling method has a light advantage regarding this aspect
0	No clear advantages or disadvantages
-1	This modeling method has a light disadvantage regarding this aspect
-2	This modeling method has a clear disadvantage regarding this aspect

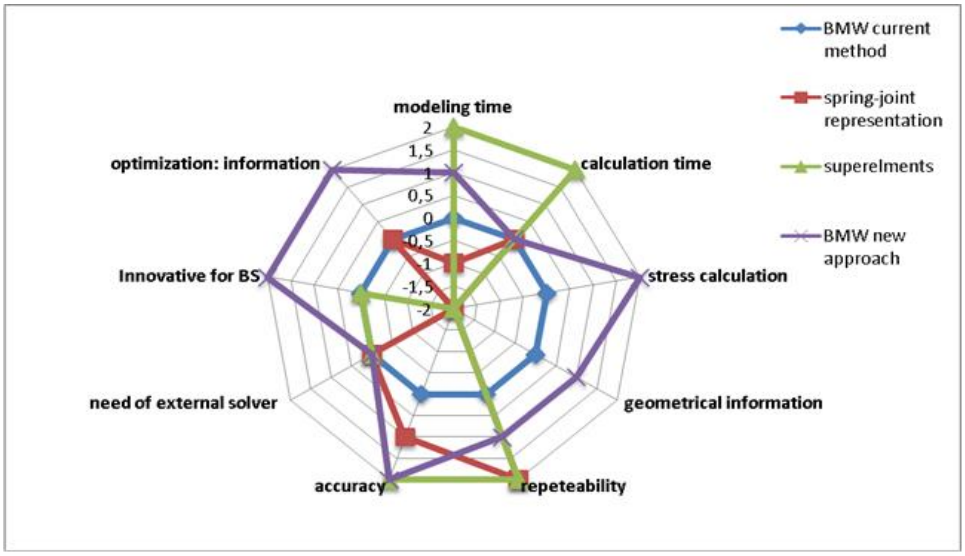

Figure 17 Summary of the evaluation of the modeling solutions

3.5 The new joint modeling approach

The new joint modeling solution proposed in the context of this dissertation is based, as already anticipated, on the hybridization of the concept model, whereby mono-dimensional beam-like FE elements are coupled with three-dimensional detailed joint structures and morphing techniques (see paragraph 3.6) are applied to the three-dimensional parts in order to realize a complete body geometrical optimization, see figure 18, the red arrows indicate the direction of motion of the control points of the morphing box.

The three-dimensional joint structures can be designed starting from the available information: sketches, full CAD models, a predecessor fine FE model, or a mixture thereof. Using FE shell elements just the thickness of the elements are available as optimization parameters, in order to overcome this problem, a morphing box is applied to the joint shell model and morphing parameters can be used as optimization control parameters. In this way a precise calculation and an optimization of the geometry can be performed in parallel.

The hybridization of the model has the potential to achieve the requested targets in terms of robustness and accuracy, while the usage of detailed shell-like structure combined with morphing applications leave the opportunity of performing geometrical multi-disciplinary optimization [4].

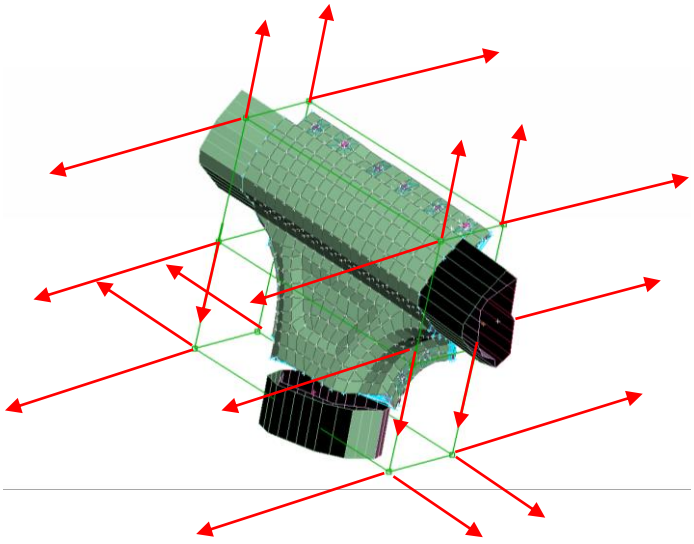

Figure 18 Hybrid-morphed concept joint

The new proposed concept model is named “Hybrid Morphing Concept Model”, it represents a more “detailed” concept modeling approach, aspects like stress calculation, geometrical optimization, connecting elements between dissimilar elements, have been investigated in order to make possible his integration in the design and optimization process.
The hybridization process has been applied to fourteen selected joints, see figure 19, playing key roles on the static and dynamic stiffness calculation.

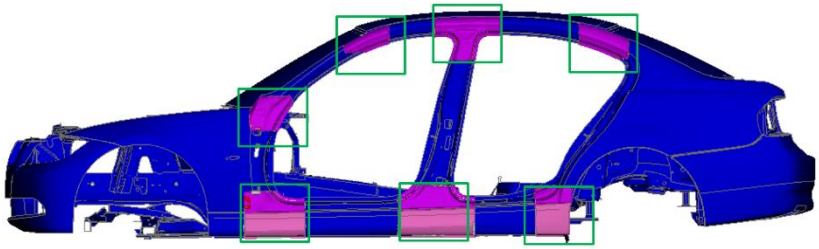

Figure 19 Selected joints for the hybridization process

Clearly the overall hybridization process increases the number of nodes of the concept model, but a relative small increase of details has the potential to assure a remarkable increase of accuracy. In figure 20 a graph shows the benefit of the hybridization process in terms of global stiffness calculation.

The current concept model with about 10000 nodes, in worst case, leads to an error on the calculation of the global stiffness up to 12% (in average 8%). Applying the hybridization, arriving to ~20000 nodes, the global error can be kept under 5% (error related to the fine FE model). Looking at pure numbers, the hybridized model has the double of nodes of the actual concept model, however from a pure computational point of view, it is not a critical aspect, the model remains anyway quick to run and to optimize. The new trend proposed, in the concept modeling design, is to increase the degree of detail, where necessary, according with the always higher calculation power available.

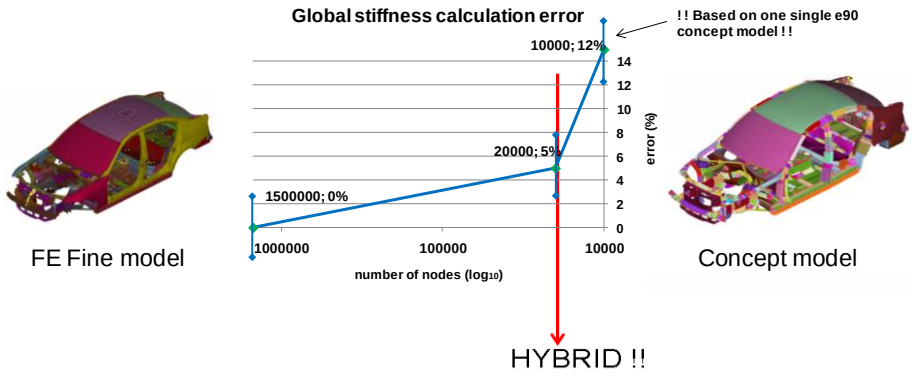

Figure 20 Global stiffness calculation error vs number of nodes of the concept model

The advantages of introducing a new hybrid concept model in the design process can be summarized as follow:

- Increase the robustness of the modeling process.
- Increase the structural performance calculation accuracy in the early design phase.
- Provide more geometrical information on the optimized joints in order to achieve the design targets.

3.6 Morphing

In this paragraph a summary of the morphing techniques available in commercial software is presented.

Morphing techniques can be grouped in two main categories: the so called “box morphing” and the “direct morphing”, the main difference consists in that in the first case, morphing actions are controlled using control points, in the second case, using design variables [15].

- The *Box Morphing* method has three different approaches.

Box Morphing - Approach A

Multiple morphing boxes that follow the shape of the structure. Moving or sliding of control points results in the morphing of the model in the desired direction. This approach allows the user to slide one part on another, or reshape a part by moving the control points of the boxes.

Box Morphing - Approach B

A single morphing box, split into many, with their edges fit on the feature lines of the model.

This approach has the following advantages:

- the surrounding boxes act as buffer zones of the morphing action, thus ensuring continuity of the deformed neighboring morphed entities.

- the ability to move the fit morphing box edges by exact translations, rotations or even snapping onto predefined target 3D curves, allows for highly controllable and precise modifications of the loaded entities. This approach is recommended for CFD models, but also for structural assemblies, when a modification of a part affects the surrounding components also.

Box Morphing - Approach C

A morphing box can handle the shape of other boxes. This approach has the following advantages:

- separate groups of morphing boxes can handle different features of the same model, without the need of complex morphing boxes.

- local and global modifications can be done of a model easily without the need of complicated script commands. This approach is recommended when local (detailed) and global modifications are needed in the same model.

- *Direct Morphing*

FE-models morphing can also be performed without morphing boxes. This can be performed either by specifying frozen/rigid nodes and morphing zones, or origin and target curves. Creating local depressions on shell mesh is also possible. This method is suggested for local modifications of a part.

The selection of the most suitable morphing technique takes into consideration mainly two factors:

- modeling time
- coupling with the optimizer

Considering that the modeling time is similar for each approach, and that the joints can be optimized independently without interact with the rest of the structures (e.g. no need for the more complex approaches B or C), the possible choices are either approach A either direct morphing.

Considering also that the "beam and shell" model is optimized using Nastran SOL200, and that ANSA, the pre-processor in use, supports the *Manual Grid Variation Method* of NASTRAN SOL200, the best morphing approach results on being the direct morphing. The approach selected supports simultaneous optimization in different directions: multiple vectoring per point and every vector can be controlled with an own design variable.

4 MODEL HYBRIDIZATION

In the previous chapter a new joint modeling approach, based on hybrid structures has been presented. The focus of this chapter is to provide the reader with a general overview on hybrid structures and more inside information on the engineering challenge of the homogenous stress calculation in structures made by dissimilar FEM elements.

4.1 Introduction to hybridization

Nowadays the most accurate method to investigate the structural performance of the thin-walled structures, like BiW, is based on detailed tridimensional shell-like structures, up to 3.000.000 nodes. In the concept phase however parameterized one-dimensional beams elements, replacing the shell-like elements, are widely used, the overall computational analysis results much quicker: ~10.000 nodes, see figure 20. Parameterized concept models give to the designer great freedom in the optimization phase, having full access to the geometrical parameters of the structure, investigating, in very short time, several topological solutions of the load-carrying structural members.

The accuracy of the concept model is far from the shell-like detailed model, the main error derives from the joint modeling based on the one-dimensional beam, and secondary from the one-dimensional model (7 DOF) of the beams [4].

Within this research activity a new concept model is propose and it is based on hybrid structures, whereby not only one-dimensional thin-walled beam elements, but also shell-like thin-walled detailed structures, are allowed. The one-dimensional FE beam elements are now coupled with three-dimensional detailed joint structures (shell-like elements) and morphing techniques are applied to the three-dimensional parts in order to realize a full body geometrical optimization, see

figure 19. The target is to increase accuracy and robustness of the actual concept model. The one-dimensional beam model used in the “beam and shell” concept model is a 7 DOF arbitrary beam cross-sections model proposed by Nastran. The beam model itself shows a good accuracy in static conditions and some limitations in dynamic analysis (local dynamic).

The introduction of shell-like elements in the concept model brings back the problem of the parameterization of the geometry of the model in order to launch optimization runs, while mono-dimensional elements provide a complete set of parameters to be optimized (height, length and thickness), in the shell-like elements just the thickness can be parameterized and therefore optimized, in order to perform a complete geometrical optimization of the shell-like three-dimensional structure of the joint, morphing techniques have been selected and applied for the complete geometrical optimization of shell-like structures, where else just the thicknesses of the shell elements would have been accessible for the optimization sequence.

Morphing techniques find a wide use in several fields, for finite element applications two main different morphing approaches are available: the so called “box morphing” and the “direct morphing”.

The “box morphing” approach is based on multiple morphing boxes that follow the shape of the structure. Moving or sliding of control points, results in the morphing of the model in the desired direction. See figure 21, in red the control points.

The “direct morphing” approach defines an origin, a target shape and the relative deformation vectors to move from the origin to the target. The final shape is controlled by design variables. See figure 22 in green, the deformation vectors.

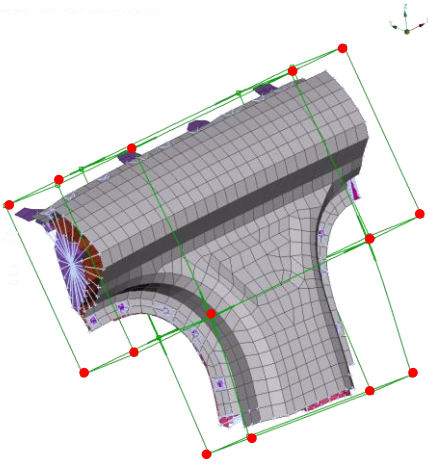

Figure 21 Box morphing approach

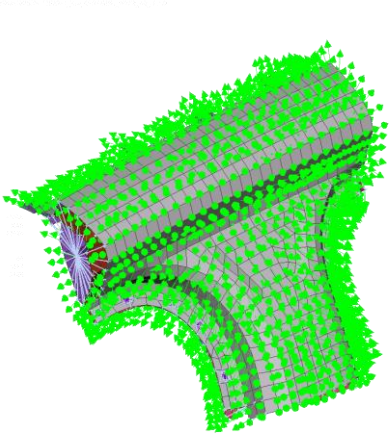

Figure 22 Direct morphing approach

The two methods are basically equivalent, except that in the “box-morphing” the actions are controlled using control points, in the other case, using design variables.

The morphing-optimization sequence is based on the *Manual Grid Variation Method*, which requires a “direct morphing” approach and avoids the usage of external optimizer. However, for a complete morphing optimization run, using direct morphing, a large number of displacement vectors need to be defined. In order to create the displacement vectors “box morphing” technique are applied. Therefore in the proposed modeling process both techniques have been applied, the “box morphing” has been used to define the deformation vectors, while “direct morphing” to control the deformations during the optimization sequence.

The displacement vectors will define the directions of the possible movements for each node of the fine model. The vectors go from an initial configuration to a final configuration, chosen by the designer. During the optimization sequence any intermediate position, along the directions of the vectors, is allowed. More in detail, shape optimization processes in Nastran, are based on the DVGRID bulk data cards. Those cards define the relation between the design variables and the grid point location. When a morphing action is performed, a nominal displacement vector is defined, from the initial to final maximal allowable position of the grid and the actual module of the vector is controlled by a design variable.

The function of the morphing box is to create appropriate deformation vectors, DVGRID, linked to the design variables that will define the final shape of the joint after optimization.

The shape and the number of the morphing boxes, influence the directions of the deformation vectors, and so have to be carefully designed, according to the optimization targets. After evaluating several configurations, the use a morphing box for each beam that has to be connected, plus one for the central part of the joint, has been selected.

An example of a simplified three-beam joint is depicted in figure 23, in this case 4 boxes have been used for a three-beam junction: boxes number 1, 3, 4 for the interfacing beams and the box number 2 for the central part. In this way it is possible, using a limited number of morphing boxes, to respect the congruency with the one-dimensional beams parameters (height, length and thickness) during optimization.

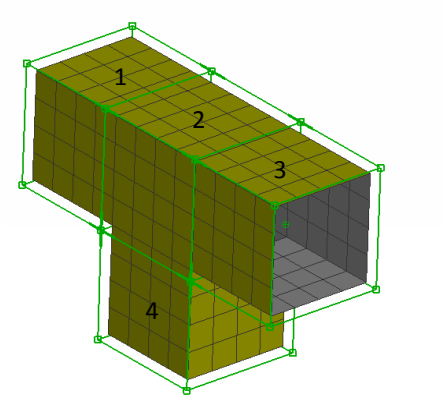

Figure 23 Example of a morphing box lay-out for a simplified joint.

The morphing techniques give the designer a broad freedom in performing any type of geometrical optimization. It is possible to perform simple morphing applications, defining an initial and a final shape of a component and controlling the intermediate position through a single design variable (scaling effect), or upgrade to more complex applications, for example assigning several design variables to different deformation vectors groups. For very complex and refined applications, it would be possible to assign a design variable to each deformation vectors or even to define multiple deformation vectors for each node controlled by multiple design variables. It is clear that the potential of morphing techniques is high, however is important to keep the right degree of complexity, if on one side a higher quality of the results can be achieved, on the other the calculation time and the interpretation of the results could become critical. In the complete concept model, depending on the optimization targets, it would be recommended for a three-beam joint, as in figure 23, to use from 1 to 4 design variables, one for each morphing box.

4.2 The engineering challenges of the hybridization

From an engineering point of view, simulating reality with hybrid structures, whereby one-dimensional elements are coupled with three-dimensional structures, is a quite complex task, (see a detailed problem clarification in paragraph 5.1). The 1D to 3D coupling in a multidisciplinary hybrid concept model based on morphing technique, leads to two main design challenges:

- Defining stress constraint parameters for consistent stress calculation between dissimilar elements.
- Defining FE structural rigorous connections between mono-dimensional elements and three-dimensional structures (formed by 2D shell elements).

The first challenge is a complex FEM application that requires a deep understanding of the theoretical background of the FEM elements and a validation phase to cross-check the quality of the application. The second is a scientific challenge and also the main target of this dissertation, exhaustively described in chapter 5 and 6.

The investigation for the selection of the appropriate stress parameters have been based on a cantilever beam, first just with closed cross sections and then also a mix of open and closed cross sections, see fig 25 and 31.

The investigations for the selection of the connecting elements have been based on simplified joint structures, like the joint in figure 23. The motivations of using models with simplified geometry are: reduced number of variables, more abstracted and generalized approach/thinking and better understanding of the cause-effect relations between the concept modeling elements and the resulting performance.

4.3 Consistent stress calculation in hybrid structures

In this paragraph the challenge of setting appropriate stress parameters for the dissimilar elements of the hybrid structures in order to reach homogenous stress results between dissimilar elements (1D-3D) is described.

The dissimilar interfacing elements in hybrid structures are mono-dimensional beams and bi-dimensional shell-like elements forming the three–dimensional structure.

The selection of the stress parameters for the homogenous stress calculation has been based on the theoretical background of the FEM manual, followed by an appropriate validation phase. For sake of completeness, some fundamental information on the beam and the shell elements employed in the model are reported, however it is clear that the following method applied to set the stress parameters in hybrid structures can be replicated with any fem code.

4.3.1 The mono-dimensional element

The beam element includes extension, torsion, bending in two perpendicular planes and the associated shears; the features are listed below [16]:

1. Distributed mass polar moment of inertia.
2. Separate shear center, neutral axis, and nonstructural mass center of gravity.
3. Arbitrary variation of the section properties (A, I1, 12, I12, J) and of the nonstructural mass along the beam.
4. Shear relief due to taper.
5. The ability to apply either concentrated or distributed loads along the beam.
6. The effect of cross-sectional warping on torsional stiffness.
7. The ability to model a beam made up of offset rods.
8. Nonlinear material properties: elastic-perfectly plastic only.

The following element forces, either real or complex (depending on the solution sequence), are output on request at both ends and at intermediate locations:

- Beam element internal forces and moments
- Bending moments in the two reference planes at the neutral axis.
- Shear forces in the two reference planes at the shear center.
- Axial force at the neutral axis.
- Total torque about the beam shear center axis.
- Component of torque due to warping.

The following real element stress data are output on request:

- Real longitudinal stress at the four points prescribed for each cross section defined along the length of the beam.
- Maximum and minimum longitudinal stresses.
- Margins of safety in tension and compression for the element if the user enters stress limits.

4.3.2 The bi-dimensional element

In FEM applications generally two different shapes of isoparametric shell elements (triangular and quadrilateral) and two different stress systems (membrane and bending) are available. There are in all a total of six different forms of shell elements that are defined, and in particular three quadrilateral element [16].

by connection entries as follows:

- Isoparametric quadrilateral element with optional coupling of bending and membrane stiffnesses.
- Isoparametric quadrilateral element with optional coupling of bending and membrane stiffness and optional mid-side nodes.
- Isoparametric quadrilateral element with no coupling of bending and membrane stiffnesses; the membrane stiffness formulation includes rotation about the normal to the plane of the element.

For the beam and shell hybrid model the first type has been chosen.

In general for this type of shell element, the forces are evaluated at the centroid of the element.

The positive directions for the stresses are shown in figure 24.

The stresses are calculated in the element coordinate system. The following real stresses are output on request:

- Normal stresses in the *x* and *y* directions.
- Shear stresses on the *x* face in the *y* direction.
- Angle between the *x* axis and the major principal axis.
- Major and minor principal stresses.
- Von Mises equivalent stress or maximum shear stress

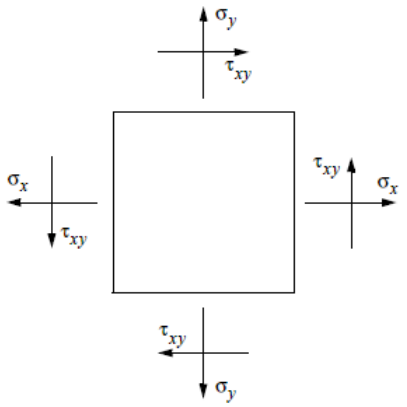

The von Mises equivalent stress for plane strain analysis is defined as follows:

$$\bar{\tau}_v = \left[1/2\left\{(\sigma_x - \sigma_y)^2 + (\sigma_y - \sigma_z)^2 + (\sigma_z - \sigma_x)^2\right\} + 3\tau_{xy}^2\right]^{1/2} \quad (2)$$

Figure 24 Stresses in shell elements

Where the strain components are defined as:

$$\varepsilon_x = \frac{\partial u}{\partial x};\ \varepsilon_y = \frac{\partial v}{\partial y};\ \gamma_{xy} = \frac{\partial v}{\partial y} + \frac{\partial u}{\partial x} \quad (3)$$

4.3.3 Selection of the stress parameters

In the shell elements, the stresses are calculated at two specified points on the cross section. The distances to the specified points are given on the property entries. The default distance is one half the thickness. The positive directions for these fiber distances are defined according to the right-hand sequence of the grid points specified on the connection.

In the beam and shell concept model the linear maximum and minimum stress in the beam elements with arbitrary cross sections is calculated at certain stress recovery points, that are automatically calculated, more likely these points are the points with minimum and/or maximum distance in the x and y direction of the section.

In order to achieve the same results for the actual concept models and the hybrids one for the stress calculation of the shell elements several solutions have

been evaluated, the final solution proposed and applied is the calculation of the stress at the corner points of each shell elements, and for each corner the sigma stress in x and y directions in both faces of the element (Z1-Z2) have been calculated.

In this case the max stress of the beam is coincident to the sigma (x) corner stress of the shell elements.

A last, but not less important note, is that the orientation of two consequent elements must be kept identical, otherwise severe errors in the stress calculation can happen.

Before applying the selected stress parameters to the full vehicle a validation phase has been performed in order to cross-check the quality of the selected parameters. The aim of the validation phase is to verify if a homogenous stress calculation between different elements of a hybrid structure is feasible.

4.4 Validation

The first step of the validation phase of the selected stress parameters consists on selecting a test structure, as simple as possible, in order to have a clear understanding of the effects of stress parameters. The structure selected is a cantilever beam.

The main idea behind this validation phase is to compare the results of a geometrical optimization of a first cantilever beam made of five mono-dimensional beams elements and a second cantilever beam, equivalent in terms of geometry, loads and constraints to the first one, whereby one of the mono-dimensional elements of the concept model is substituted with shell-like elements and morphing vectors are applied, creating an hybrid structure.

The objective function of the optimization sequence is defined in such a way that the stress level after optimization in the five sections of the two beams must be constant. In this way after the optimization sequence the two beams should have the same geometry; divergences on the results will indicate a wrong selection of the stress parameters in the hybrid structure.

The validation process has been replicated two times, the first time using closed sections and the second time using open sections, in order to investigate the quality of the stress parameters selected also in case of warping phenomena.

In the following paragraphs the most relevant results of the validation phase with a deeper insight on the stress calculation approach is presented.

4.4.1 Validation of the hybrid model with closed sections

The validation process started creating a hybrid cantilever beam structure and then comparing it with a reference one, non-hybrid, using rigid connection elements in static and dynamic conditions. The second step consists on optimizing the two structures and comparing the optimization results, hybrid versus non hybrid.

The reference structure has been modeled like the “beam and shell” concept model, using mono-dimensional beams with arbitrary beam cross sections see figure 25 a second one hybrid, equivalent to the first, whereby one of the beam element has been replaced with shell elements and morphing vectors, see figure 27. The design model is based on five design cards, five variables controlling the five heights of the beam elements, the same for the hybrid structures where the displacement of the shell elements are guided with vectors, created using morphing boxes. A single force has been applied at one end of both structures and at the other end the three displacements and the three rotations have been constrained. The design objective is the weight and there are two types of constraints, the max displacement allowable at the extremity where the force is applied and the max stress allowable for each beam. Before the optimization run, a static calculation and a cross-check of the deformations of the extremities of the two beams have been done. The results of the optimization run for the two beams are reported in figure 29, for each beam all the five design variables called H1-H2-H3-H4-H5 are listed, see figure 25 and 27, the focus of the investigation is on the comparison of the design variable H3.

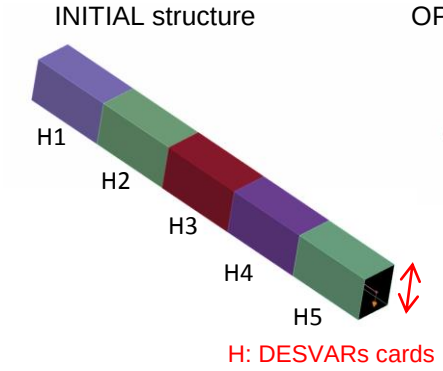

Figure 25 Reference beam

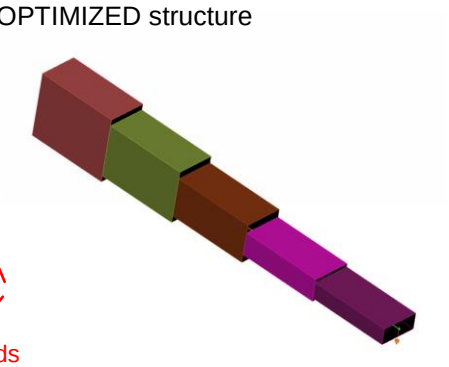

Figure 26 Reference beam optmimized

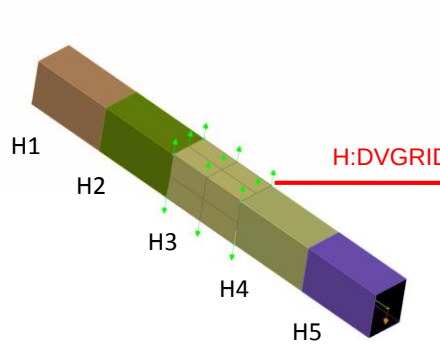

Figure 27 Initial hybrid beam

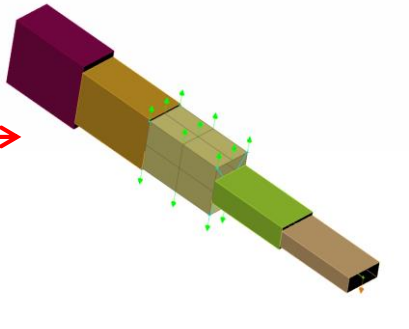

Figure 28 Optimized hybrid beam

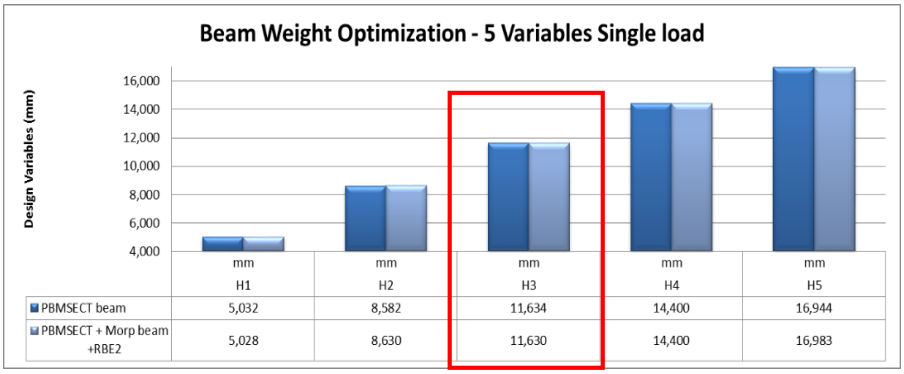

Figure 29 Results of the optimization run – single load

The results of the optimizations show that the five variables of the hybrid structure (connected with RBE2 elements) reach basically the same values of the reference one, the first step of the validation phase has a positive outcome.

The next step of the validation phase is to repeat the same test, loading the structures with loads in multiple directions. Two perpendicular forces and a moment have been applied to the free end of the beam. Stress and displacement constraints have been kept constant as in the previous case. After a cross-check of the deformations of the two beams (static calculation), an optimization run has been launched. The design objective is again the weight. The result of the optimization are reported in figure 30.

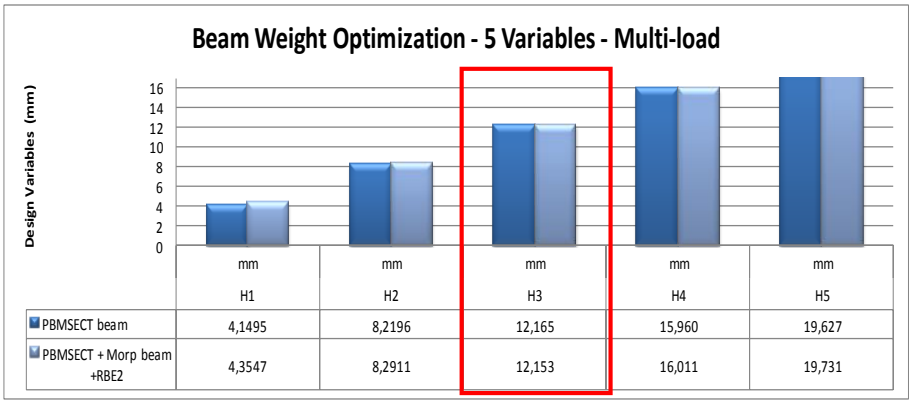

Figure 30 Results of the optimization run – multi-load

The results are in line with the expectations, all the five variables have been optimized at the same values including the variable H3. The second phase of the validation process has also a positive outcome.

4.4.2 Validation of the hybrid model with open sections

The next step of the validation phase is to cross-check the result of this approach in case of open sections in order to verify the quality of the selected stress parameters in case of warping phenomena.

As for the closed sections, first a single-load test case has been verified, then a multi-load case.

Designing open sections, warping coefficients have to be assigned to the mono-dimensional elements, open section members, such as channels, undergo torsion as well as bending when transverse loads act anywhere except at the shear center of a cross-section. [16] This torsion produces warping of the cross-section so that plane sections do not remain plane and, as a result, axial stresses are produced. This situation can be represented in the following differential equation for the torsion of a beam about the axis of shear centers:

$$G\frac{d}{dx}\left(J\frac{d\theta}{dx}\right) - E\frac{d^2}{dx^2}\left(C_w\frac{d^2\theta}{dx^2}\right) = m \tag{4}$$

Whereby:

E = Young's modulus of elasticity
C = Warping constant
G = Shear modulus
J = Torsion constant
Θ = Angle of rotation at any cross-section
m = Applied torsional moment per unit length

The reference structures is shown in figure 31, while the hybrid one in figure 32.

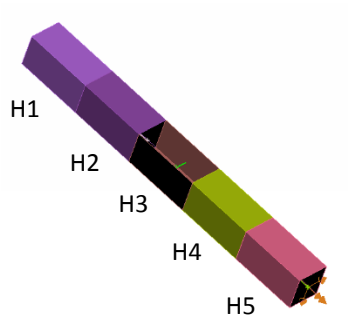

Figure 31 Reference beam with an open section

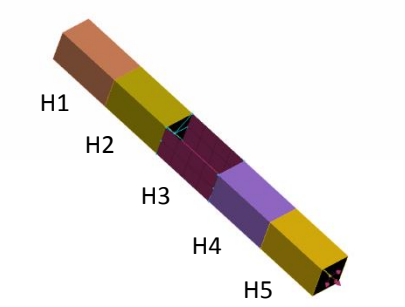

Figure 32 Hybrid beam with an open section

In this case the two central sections of the beams are open-sections, either in the reference beam, figure 31, or in the hybrid beam, figure 32.

The design models are the same as in previous case (see par. 4.4), they are based on five design cards, five variables controlling the heights of the beams for both models, H1, H2, H3, H4, H5. The design objective is, as in previous case, the weight and there are two types of constraints: the maximum displacement allowable at the free extremity and the maximum stress allowable for each beam. As in previous test a single force has been applied at one end of both structures and at the other end the three displacements and the three rotations have been constrained. In figure 33 the results of the optimization are shown. Also with open sections the results are in line with the expectations, all the 5 design variables have a minimum difference. The third phase of the validation process has also a positive outcome.

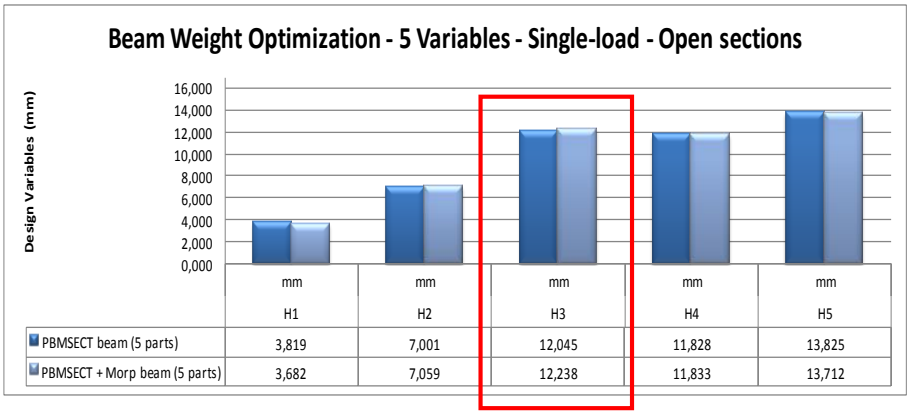

Figure 33 Results of the optimization run – single-load – open sections

The final study case is the comparison of the same two structures shown in figures 31 and 32, loaded with multiple directions loads: two perpendicular forces and a moment in the direction of the beam axes have been applied to the free end of the beam.

The design models are also equal to the previous case and are based on five design variable controlling the heights of both beams.

The design objective, as in previous cases, is the weight and there are two types of constraints: the max displacement allowable at the extremity where the force is applied and the max stress allowable for each beam. The results of the optimization proposed by the gradient based solver for both structures are shown in figure 34, the results are again in line with the expectations.

The final phase of the validation process has also a positive outcome.

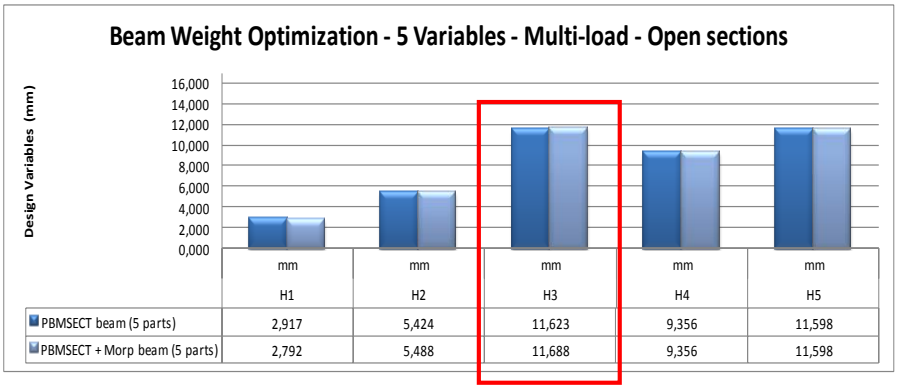

	mm H1	mm H2	mm H3	mm H4	mm H5
PBMSECT beam (5 parts)	2,917	5,424	11,623	9,356	11,598
PBMSECT + Morp beam (5 parts)	2,792	5,488	11,688	9,356	11,598

Figure 34 Results of the optimization run – multi-load – open sections

4.5 Conclusions

The selected stress parameters described in paragraph 4.3.3 are suitable for performing homogenous stress calculation in the hybrid structures, whereby one-dimensional thin-walled beam elements with arbitrary cross-sections are combined with shell-like thin-walled detailed structures.

5 CONNECTING DISSIMILAR FE ELEMENTS

In this chapter a fundamental property of the center of mass of cross-sections of beam structures, defined within this research activity, is presented. Starting from the above mentioned fundamental property, going through the principle of virtual work, a set of congruency equations for the rigorous connection of dissimilar FEM elements for hybrid thin-walled structures, whereby one-dimensional elements are coupled with three-dimensional joint structures, are defined.

5.1 Problem clarification

The main challenge, realizing hybrid structures, lies on the design of the connection of the interfacing cross sections, between the shell-like detailed structure and the one-dimensional beams, see figure 35, [17] [18] [19] [20] [21] [22] [23] [24] [25] [26] [27] [28] [29] [30] [31] [32] [33] [34] [35] [36] [37] [38] [39] [40] [41] [42] [43].

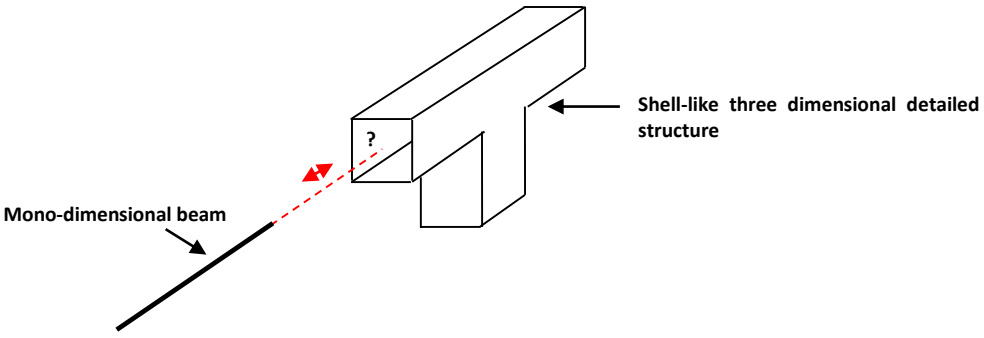

Figure 35 Dissimilar elements to be connected in hybrid structures

The interfacing cross section of a detailed shell-like structure has sufficient degrees of freedom to entirely describe the behavior of a cross section of a thin walled structure, that is able of rigid translations (x, y, z), rigid rotations (Θx, Θy, Θz), warping ω (out-of-plane deformations), and distortion χ (in-plane deformations). A good representation of possible deformations of the interfacing cross sections is given by an 8 DOF model, depicted in figure 36.

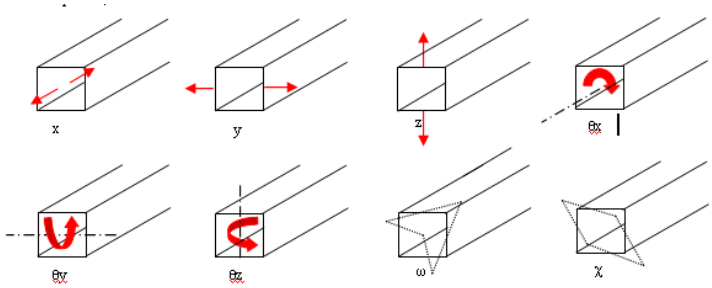

Figure 36 Deformations of the couture of a thin-walled beam with 8 dof

On the other side the 7 DOF one-dimensional beam model (7 is the highest number of DOF available in commercial software) describes the six rigid motions of the cross section, as represented in figure 37, through the three rigid translations (x, y, z), the three rigid rotations (Θx, Θy, Θz), and it takes into account the effect of the warping of the sections (7th DOF) by a correction factor Cw, see formula (10), that correlates the applied moment to the rotational axial displacement of the beam.

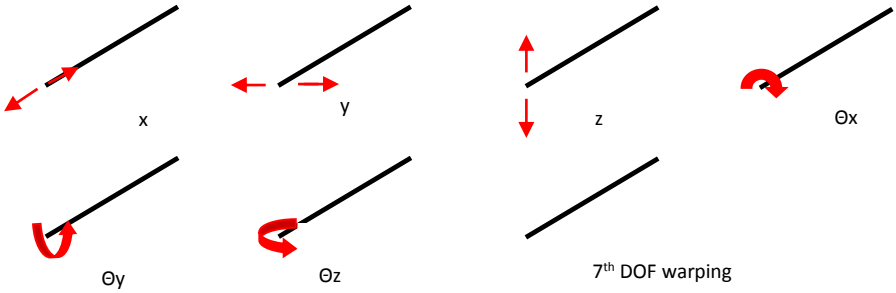

Figure 37 Representation of the 7th degrees of freedom of the interfacing nodes of a one-dimensional beam .

Here the formula:

$$m_0 = \frac{d^2}{dx^2}\left(EC_w\frac{d^2\theta_x}{dx^2}\right) - \frac{d}{dx}\left(GJ\frac{d\theta_x}{dx}\right) \quad (5)$$

The Cw factor is calculated based on the actual geometry of the cross section of the beam.

The two interfacing cross sections of a hybrid model have clearly different modeling and mathematical structures; the connection strategy between dissimilar elements (targeting 0% error in terms of virtual work) is an engineering challenge. Applying the available standard FE connecting elements (e.g. RBE3), an error, depending on the boundary conditions, is introduced. In order to find a solution, an extensive search on the existing “prior art” has been done and reported below.

5.2 Connecting elements: “prior art” and “state of the art”

In this section a detailed description of the prior art in terms of connecting elements available in commercial software or in literature is presented. What the author also consider the “state of the art” is presented in a dedicate paragraph below.

5.2.1 Rigid connections

The rigid connections define a rigid body whose independent degrees of freedom are specified at a single grid point and whose dependent degrees of freedom are specified at an arbitrary number of grid points, see figure 38 [16] [34].

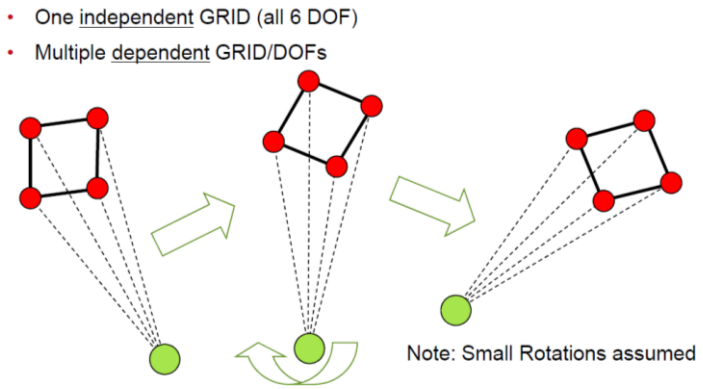

Figure 38 Rigid connection governing equations representation

The rigid connections have the following characteristics:

- Elements stiffen locally the cross sections, no warping or distortion is allowed → an error is eventually introduced.
- Easy to implement.
- Intuitive to understand: the displacement of the independent node is directly transferred to the dependents nodes, the force depends on the deformation of the sections/beams → suitable to describe internal forces.
- The moments and forces transferred trough the independent node do not depend on the relative position of the nodes.

- No local moments are applied on the dependent nodes.

It is important to notice that in case that the cross-section to be connected are warping and distortion free, the rigid connection guarantees a 0% connection error. In all the other cases an error, eventually relevant, is introduced, see benchmark results in paragraph 5.3.

5.2.2 Interpolating connections

The interpolating connecting element defines the motion at a reference grid point as the weighted average of the motions at a set of other grid points [16] [34].

For a better understanding of the governing equations, please refer to figure 39.

The interpolating connections have the following characteristic:

- Elements do not stiffen locally the cross sections.
- Not intuitive.
- The independent nodes can be “weighted”.
- Moments and forces transferred trough the dependent node, depend on the relative position of the nodes.
- Not recommended for transferring moments.
- If no weighting factors are applied then the forces are homogeneously distributed on the independent nodes.
- If the interpolating connection is applied on three aligned points then it needs rotational constraints.

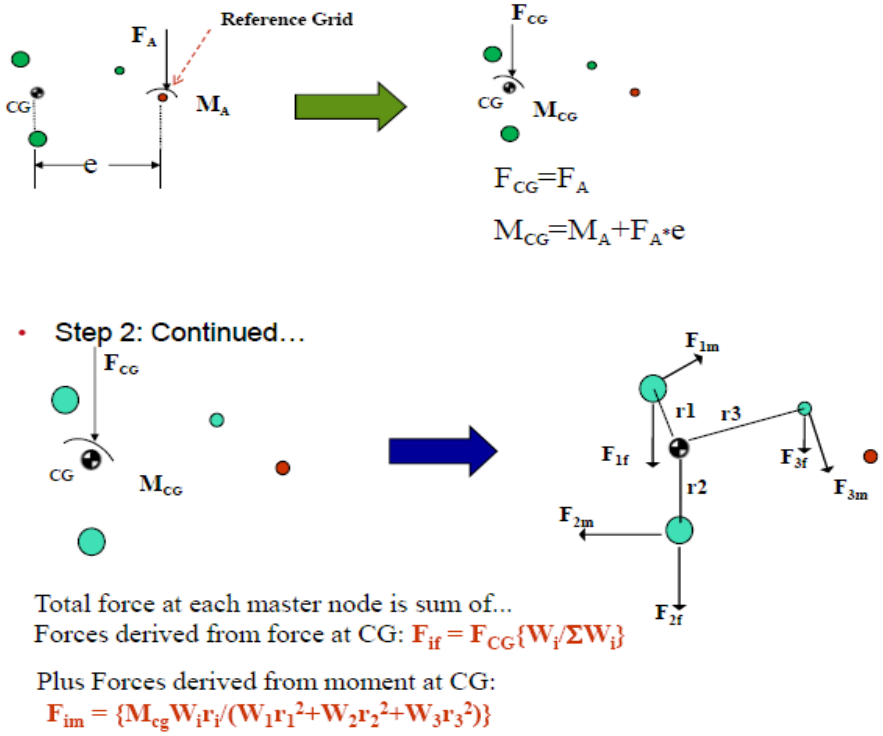

Figure 39 Interpolating connecting elements governing equations representations [34]

In general the interpolating connections are not suitable for connecting dissimilar elements, relevant errors occur systematically, see benchmark results in paragraph 5.3.

5.2.3 Advanced connecting element: RBE 2.5

The main idea is to create a trade-off between a rigid and an interpolating connection, see figure 40, [11].

The so called RBE 2.5 characteristics can be summarized as follows:

- The element does not stiffen locally the cross sections.
- Complex to implement (many parameters have to be defined).
- A general implementation strategy has to be defined (e.g. number of connecting points, number of interpolating connections to be used, number of connecting points etc.)-> Hard to characterize from a mathematical and physical point of view.

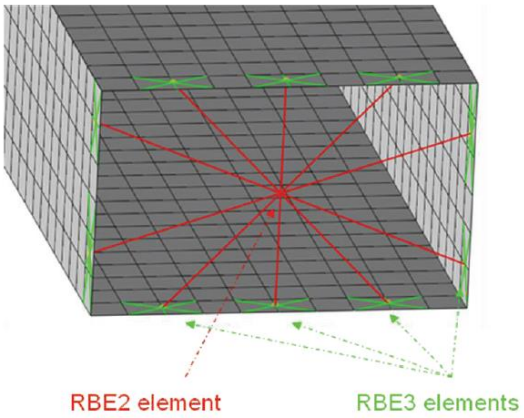

Figure 40 RBE 2.5 connection

Even though it has been proved that the RBE 2.5 connections in certain specific conditions provide a connecting error close to 0%, in general they are not suitable for an omni-comprehensive applications, relevant connecting errors can be identified depending on the boundary conditions, see benchmark results in paragraph 5.3.

5.2.4 Advanced connecting element: RBE2 + CELAS

It is a rigid connection connected to the shell-like structure using spring elements, so called RBE2 + CELAS, developed within this research activity, see figure 41.

- The connection allow warping and distortion of the section.
- Need a tuning of the spring depending on the material properties and load conditions.
- In case of zero warping and zero distortion introduces an error.
- A general implementation strategy has to be defined (number of connecting points, type of spring elements, stiffness of the spring elements etc.).

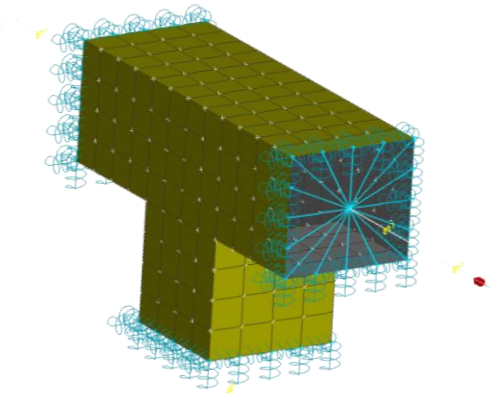

Figure 41 Simplified joint with RBE2 + CELAS

It has been proved that the RBE2 + CELAS connections, in certain specific conditions, provide a connecting error close to 0%, but in general they are not suitable for an omni-comprehensive applications, relevant connecting errors can be identified depending on the boundary conditions, see benchmark results in paragraph 5.3.

5.2.5 Multi-point constraint equations

Multi-point constraint equations can be used in any FEM software to create any type of linear polynomial relationships between N nodes of a structure, it is a powerful tool and has a wide area of application [16].

5.2.6 Connecting elements: “state of the art”

What the author considers the “state of the art” of the connecting elements is an interesting mathematical solution for matching dissimilar elements in hybrid structures, based on the principle of virtual work, proposed by the authors Kim and Kim.

The connecting element expresses the congruency of the displacement between a one-dimensional beam with 8 DOF, specifically developed and implemented by Kim and Kim, and a detailed FE shell-like three-dimensional structure.

Here an introduction to the Kim and Kim approach and a critical review, [17] [18] [19] [20] [21] [22] [23] [24] [25] [26] [27] [28] [29] [30] [31] [32].

“Kim&Kim” approach:

In the “Kim&Kim”’s approach a detailed joint region as shown is figure 42 is connected to three 8DOF mono-dimensional beams, the congruency equations of the interfacing elements are calculated equalizing the virtual work of the two interfacing elements.

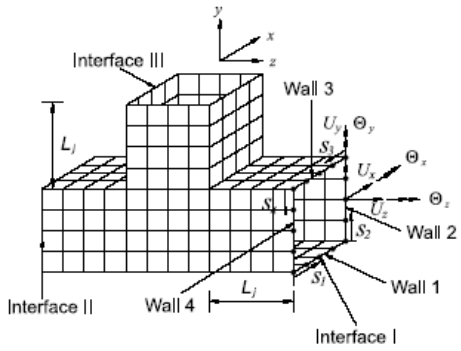

Figure 42 Model of the joint region

The equations proposed by Kim&Kim have the following structure:

$$U_{x_i}^{\mathrm{I}} = u - y_i\theta_z + \frac{bh}{b+h}\left\{\frac{4h}{b}\left(\frac{y_i}{h}\right)^3 - \left(\frac{h}{b}+2\right)\left(\frac{y_i}{h}\right)\right\}\chi \tag{6}$$

$$U_{y_i}^{\mathrm{I}} = v + \frac{b}{2}\theta_z + \frac{bh}{b+h}\chi \tag{7}$$

$$U_{z_i}^{\mathrm{I}} = w + y_i\theta_x - \frac{b}{2}\theta_y + y_i\frac{b}{2}\omega \tag{8}$$

$$i = 1 + N_1^{\mathrm{I}}, \ldots, N_2^{\mathrm{I}} \tag{9}$$

Where U_i is the displacement respectively along x,y,z of each node of the shell-like structure expressed in function of the displacements of the interfacing node of the one-dimensional beam (u,v,w), plus terms related to the warping integral function ω and to the distortional integral function χ, describing the cross sectional deformation status. The integral functions are solved for each 8DOF mono-dimensional beam, and then calculated and coupled for each node of the shell-like interfacing cross section.

Critical review of the "Kim&Kim" equations:

the "Kim&Kim" equations define univocal relations between the interfacing node of the one-dimensional beam and the nodes of the shell-like detailed three dimensional interfacing structure. The deformation status of the shell-like cross section is equalized to the rigid motion of the interfacing node of the one-dimensional beam, plus the warping integral function ω and the distortional integral function χ (approximated function) are introduced. Any approximation/error on the distortional function has a direct impact on the position of the shell like nodes, introducing an error.

A validated global analytical solution describing the distortional deformation of arbitrary thin-walled beam cross sections does not exist, in literature analytic precise solutions are proposed only for simple cross-sections (e.g. square or circular shape). The distortional integral χ function is therefore defined using a semi-analytical approach, based on the modal analysis of the interfacing cross sections. The idea is that the cross sections will deform, depending on the boundary conditions, following their own first or the second mode shape. The critical point is that, it has to be identified "a priori" the operational conditions and which mode shape the beam will follow.

The warping integral function ω is calculated based on the Alte Gjelsvik formulation. The integral constant and a pole of the function have to be defined.

In general the “Kim&Kim” approach is a precise method, but there are several drawbacks:

- It is quite complex to set up.
- It is suitable for 8DOF beam models.
- The distortional integral χ function is defined only for simple cross-sections (e.g. square or circular shape) and certain boundary conditions.
- The adaptation to a 7DOF beam (eliminating the distortional function from the formulation, in case of arbitrary cross-section), leads to a connection very similar to a rigid connection, and will not carry any valuable reduction of the connecting error.

Considering those drawbacks, it appears clear that the “Kim&Kim” solution, even though is a sophisticated mathematical solution, is not yet universally applicable for concept modelling applications, a different/new solution is needed.

5.3 Benchmark of connecting elements

The dissimilar interfacing cross sections of a hybrid model have different mathematical structures, the best connection strategy between dissimilar elements, targeting 0% error, is not known. Using the available connecting elements, an error depending on the boundary conditions could be introduced, in order to find the best solution, a benchmark activity, evaluating the performance of the available connecting elements has been done, the details are given below.

Ideally the dissimilar interfacing cross sections should be coupled in a continuous way, capable of transferring internal forces without any error in static and dynamic simulations. The shell-like interfacing cross section has to be connected with a mono-dimensional element with 7 DOF that transfers the 3 displacements, 3 rotations, the warping related function, and should be still able to let the shell-like cross-section eventually deform in-plane.

The shell-like interfacing cross section has to be connected with an element that can transfer the 3 displacements, the 3 rotations, the warping related function, and should be still able to let the shell-like cross-section eventually deform in-plane, (distortion); so a certain “elasticity” of the connecting element is necessary.

In order to evaluate objectively the results of the benchmark activity, the problem is posed in a measurable way, comparing the displacements of key points

of the hybrid structure, connected with selectively different connecting elements, with the displacements at corresponding points of a shell-like reference model and a standard concept joint model with arbitrary beam cross-sections ABCs (designed according to the current BMW standards), under different load conditions. The three concept models are shown in figure 43.

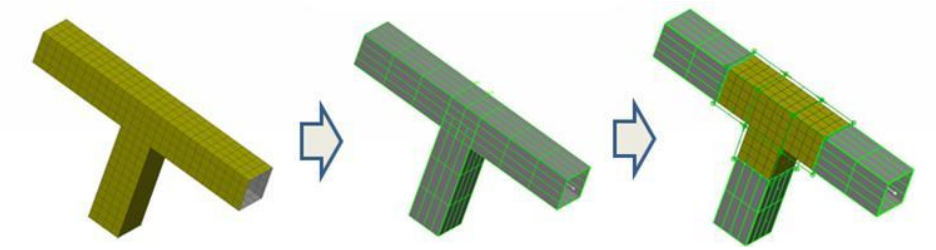

Figure 43 Simplified joint structures investigated for the benchmark activity

Two extremities of the shell-like reference model have been fully constrained using rigid connecting elements, and the force on the third free extremity has been applied through a multi-point rigid element. Regarding the hybrid structure and the concept ABCs structure, the constraints and forces have been applied directly on the nodes of the mono-dimensional beams. Three load cases have been chosen for the static analysis; they are displayed in figure 44: a vertical force Fz, a lateral force Fy, and a moment along the x axes Mx.

For each load condition the main displacement of the free extremity has been measured and compared. In the hybrid model the following connecting elements have been tested:

- Rigid (all nodes connected)
- RBE2.5 made of 1 RBE2 and 4 RBE3 (configuration 1)
- RBE2.5 made of 1RBE2 and 8 RBE3 (configuration 2)
- RBE2 plus 48 CELAS elements.

The three load conditions have been specifically selected in order to create 3 specific deformation statuses of the interfacing cross sections:

- Case 1: rigid motion of the cross section without warping or distortion
- Case 2: rigid motion of the cross section without warping but distortion
- Case 3: rigid motion of the cross section with warping and distorion

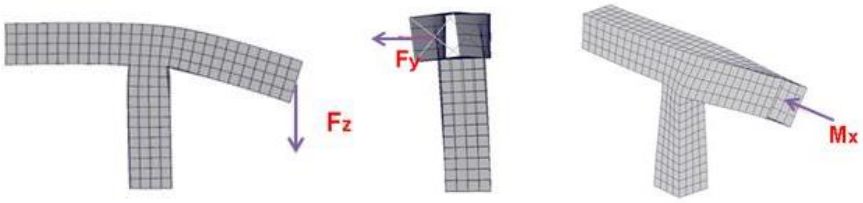

Figure 44 Load cases selected for the benchmark activity

The structural dynamic performances of the joints have not been investigated, the reason is that a hybrid structure made of few mono-dimensional 7DOF beam elements, is not suitable for precise calculation of the dynamic performance. In case of large structures, with more of 1000 mono-dimensional elements, whereby the effect of local distortion and distortional warping are negligible, structural dynamic performance can be evaluated.

In order to proceed analyzing the most suitable connecting solution, a consideration on the possible source of error in the model are necessary.

The overall error will be partially due to the quality of the beam model used, and partially to the connection type, however the error related to the type of beam is very low, below 0,5%, therefore it can be considered not relevant.

5.3.1 Results of the benchmark of the connecting elements

In order to find the most suitable connection, the following connecting elements: RBE2, RBE3, RBE2.5 (configuration 1 and 2), RBE2+CELAS, have been investigated and benchmarked. The results are reported in the following figure 45.

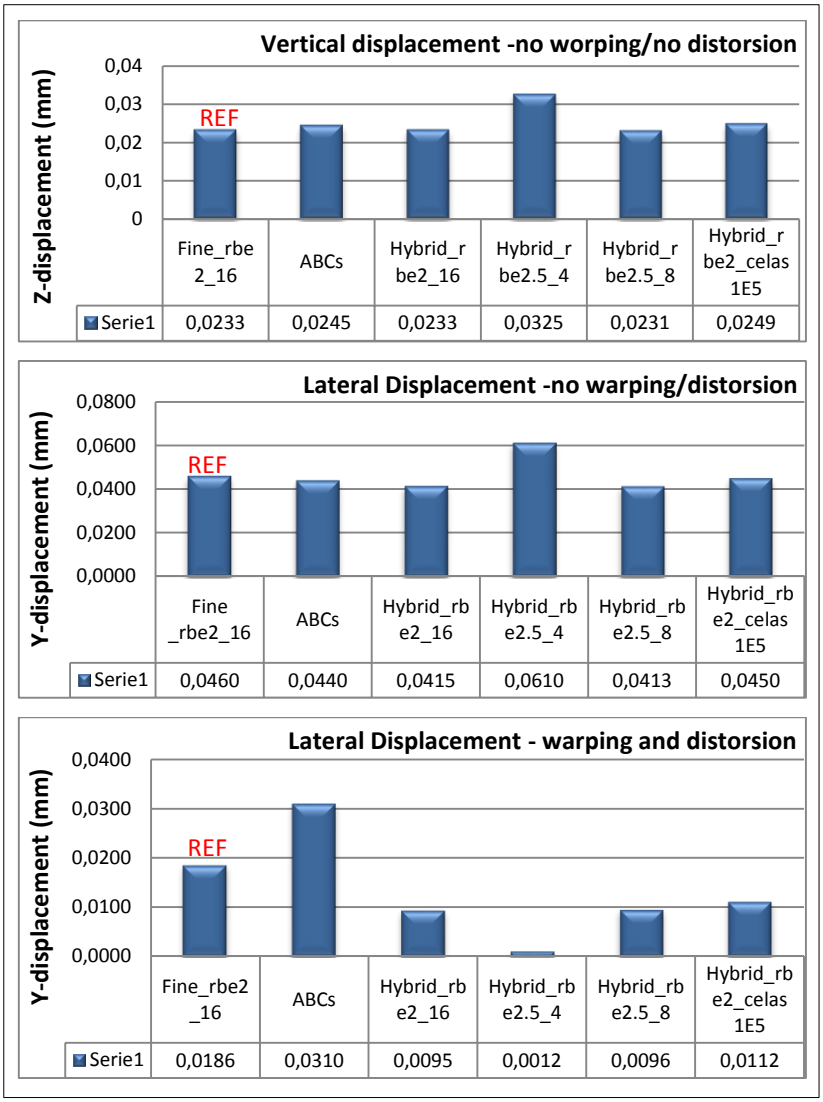

Figure 45

The rigid connection RBE2 performs well (~0% error) in case of no warping and no distortion of the cross sections, while the elastic solutions should be preferred in case the warping and distortion deformations of the cross sections assume values comparable with the rigid motion of the sections. The current BMW model based on an empirical combination on one-dimensional beams with arbitrary cross sections provides good results in case of zero warping and low distortion level.

In general the distortional level of the sections of the concept model is low, however the critical aspect of the concept ABCs modeling approach is that it depends on the subjective interpretation of the designer, therefore it is difficult to realize consistently precise models of geometrically complex joints.

The rigid connection RBE2: provides top result (~0%) in case of zero warping and zero distortion. In case of deformation of the cross sections there is relevant stiffening of the section. Considering that in general the deformation level of the section of the concept model is low, it could be considered as a possible solution.

The deformable connection RBE 2.5: with a good tuning (e.g. RBE2.5 made of 1 RBE2 and 8 RBE3) in specific cases good results can be achieved, otherwise not suitable for the concept modeling applications. Additionally the internal forces are transferred through RBE3 elements, difficult to control, especially during optimization.

The deformable connection RBE2+CELAS: globally, in this case it is the benchmark, provides best results, it is a trade-off solution. However a specific tuning of the stiffness of the spring elements is needed for each application, thus not suitable for concept modeling. This connection type can handle well any type of sectional deformation, but the critical aspect is that in case of zero warping and distortion introduces an error.

In conclusion no one of the available connections fully satisfy the expectations in all boundary conditions. In order to select the best connecting element, it is necessary to define which type of deformation are dominant in the concept model, more precisely it is necessary to define the order of magnitude of the deformations in the BiW model in the interfacing cross section under operating conditions. Once the dominant deformations (rigid, out/in plane) have been defined it is possible to define the most suitable connecting element.

Using those connections it has to be defined if, in the complete concept model, rigid or elastic connections have to be implemented, or rather which types of deformations are dominant (rigid vs warping/distortion).

A new solution for the rigorous connection of dissimilar FEM elements for hybrid (car body) thin-walled structures, developed within this PhD research activity, is presented in the next paragraph 5.5.

5.4 Fundamental property of the centre of mass and congruency equations for rigorous connections

The idea hereby proposed, is to derive the congruency equations equalizing the virtual work done by the interfacing one-dimensional cross section to the virtual work done by the nodes of the interfacing three dimensional cross section, defining the rigid motions of the interfacing node of the one-dimensional beam as function of the motions of all the nodes of the interfacing shell-like cross section. The authors “Kim&Kim” define the congruency conditions, expressing the displacement of each node of the shell-like structure as function of the displacements of the interfacing node of the one-dimensional beam, plus the relative local values of the complex integral functions of warping and distortion.

Reversing the “Kim&Kim” equations, expressing the displacements of the interfacing node of the one-dimensional beam as function of the displacement of each node of the shell-like structure and applying the fundamental property of the centre of mass of the cross-sections established within the framework of this research activity, it is possible to define a radically simple system of congruency equations.

The congruency equations for the rigorous connection of dissimilar FEM elements for hybrid (car body) thin-walled structures, whereby one-dimensional elements are coupled with three-dimensional joint structures are hereby presented.

Let us consider a 7DOF hybrid beam like in figure 46 and a global coordinate system right-handed (x,y,z), where the z axe is parallel to the beam axis.

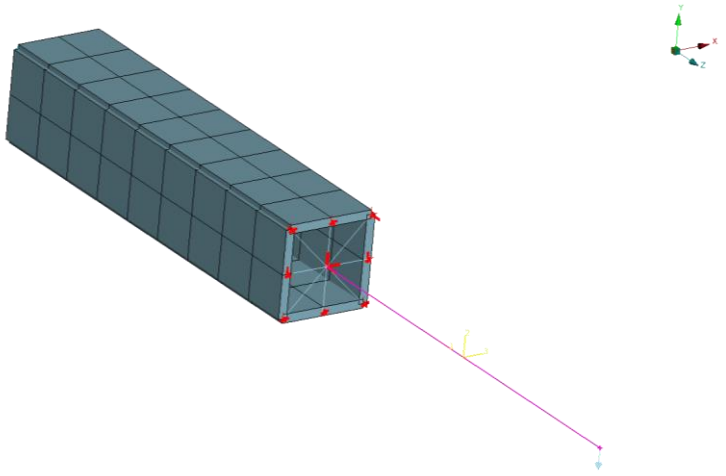

Figure 46 Hybrid beam: shell-like structure coupled with one-dimensional beam

Let us define the one-dimensional beam displacement components of the interfacing node as *(u, v, w, ϑx, ϑy, ϑz, Cω)*

whereby Cω is the warping coefficient and the displacement components of the general node i (i=1…N) of the shell-like detailed structure of the interfacing cross section as $(Ux_i, Uy_i, Uz_i, \alpha_i, \beta_i, \gamma_i)$.

The structure is a cantilever beam, with the left extremity constrained using a rigid connection RBE2 (123456) at the centre of mass of the cross section-> warping restrained.

The displacements along x of the generic node i (i=1…N) of the interfacing shell-like cross sections, can be written as follow:

$$U_{xi} = u_i + y_i \vartheta_z + F\chi_i \tag{10}$$

(rigid motion of the connecting point + rotation + distortion)

Summing the equations for all the N nodes of the interfacing cross section:

$$\sum U_{xi} = \sum u_i + \sum y_i \vartheta z + \sum F\chi_i \tag{11}$$

Being u_i equal for all the nodes

$$\sum U_{xi} = Nu_i + \sum y_i \vartheta z + \sum F\chi_i \tag{12}$$

If the connecting point of the interfacing cross sections u_i is defined as the center of mass of the cross section, u_i can be written u_{cm}

The center of mass is defined as:

$$Cm_x = \sum m_i x_i / \sum m_i \tag{13}$$

Where x_i is coordinate of the i-node along the x axis

$$m_i = \rho_i A_i \tag{14}$$

ρ_i = density associated to the i-node

A_i: area around the i-node, proportional to the mesh dimension and so that $\sum A_i$ = total area of the cross section

$$Cm_x = \sum \rho_i A_i x_i / \sum \rho_i A_i \tag{15}$$

After deformation

$$Cm_x + u_{cm} = \sum (\rho_i A_i x_i^{After\ Deformation}) / \sum \rho_i A_i = \sum (\rho_i A_i (x_i + U_{xi})) / \sum \rho_i A_i \quad (16)$$

That can be expressed as

$$Cm + u_{cm} = (\sum \rho_i A_i x_i + N \rho_i A_i u_i + \sum \rho_i A_i y_i \vartheta z + \sum \rho_i A_i F\chi_i) / \sum \rho_i A_i \quad (17)$$

the displacement of the center of mass is

$$u_{cm} = \sum (\rho_i A_i U_{xi}) / \sum \rho_i A_i = (\sum \rho_i A_i u_i + \sum \rho_i A_i y_i \vartheta z + \sum \rho_i A_i F\chi_i) / \sum \rho_i A_i \quad (18)$$

$$u_{cm} = (u_{cm} \sum \rho_i A_i + \sum \rho_i A_i y_i \vartheta z + \sum \rho_i A_i F\chi_i) / \sum \rho_i A_i \quad (19)$$

$$u_{cm} \sum \rho_i A_i = u_{cm} \sum \rho_i A_i + \sum \rho_i A_i y_i \vartheta z + \sum \rho_i A_i F\chi_i \quad (20)$$

proving that

$$\sum \rho_i A_i y_i \vartheta z + \sum \rho_i A_i F\chi_i = 0 \quad (21)$$

If the connection point of the one-dimensional beam is defined as the instant centre of mass of the shell-like cross section (homogeneous and non-homogeneous sections with an arbitrary distribution of nodes), automatically the weighted contributions of the warping, distortions and rotations, cancel each-other, avoiding to calculate the integral deformations functions ω and χ of the cross sections in order to establish the congruency conditions. This is the fundamental property of the centre of mass of the beam cross-sections, defined within this research activity, essential to define the following congruency equations.

the final equations can be written as

$$u_{cm\text{-}x} = (\sum \rho_i A_i U_{xi}) / \sum \rho_i A_i \quad (22)$$

The same procedure has been applied for the U_y, U_z, obtaining

$$v_{cm\text{-}y} = (\sum \rho_i A_i U_{yi}) / \sum \rho_i A_i \quad (23)$$
$$w_{cm\text{-}z} = (\sum \rho_i A_i U_{zi}) / \sum \rho_i A_i \quad (24)$$

In order to define congruency relations between the angles, it is possible to proceed as above, defining the balance of the virtual work between the rotations of the interfacing cross-sections.

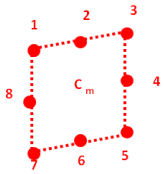

(u,v,w) x N

Figure 47 Nodes of the shell-like cross section

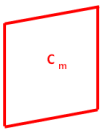

(u,v,w, θx, θy, θz)

Figure 48 1-D rigid cross-section

The rigid rotations of the one-dimensional beam cross-section (θx, θy, θz, see figure 48) can be defined as the weighted average of the rotations of the N nodes of the shell-like sections around the respective x',y',z' axes passing by the Cm (see figure 47).

In figure 49 a representation of the calculation approach of the angle β for the i-node is shown. The angle is defined as

$$\beta = arctg\ U_z/d \tag{25}$$

that for small angles can be written as

$$\beta = U_z/d \tag{26}$$

whereby d is the distance along x between the node and the vertical axis passing by the Cm.

More in detail the angles are defined for any node of the cross section and then averaged, the calculation approach can be described as it follows

$$\alpha_i = U_{zi}/d_{xi} \tag{27}$$
$$\beta_i = U_{zi}/d_{yi} \tag{28}$$
$$\gamma_i = U_{xi}/d_{zi} + U_{yi}/d_{zi} \tag{29}$$

where d_x,d_y,d_z, are the respective distances of the I node form the x',y',z' axes passing by the Cm

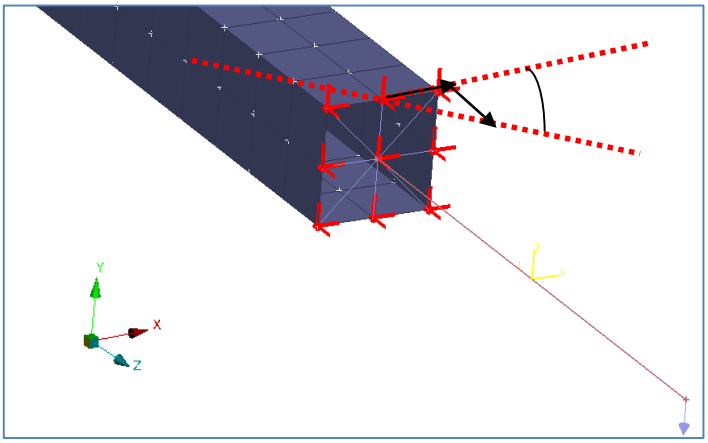

Figure 49 Representation of the calculation approach of the angle β for the i-node

Following this approach for the relations between the angles of the connecting point of the mono dimensional beam and the rotations of the shell-like cross section can be defined as:

$$\vartheta x = (\sum \rho_i A_i (U_{zi}/ d_{xi}))/ \sum \rho_i A_i \quad (30)$$
$$\vartheta y = (\sum \rho_i A_i (U_{zi}/ d_{yi}))/ \sum \rho_i A_i \quad (31)$$
$$\vartheta z = (\sum \rho_i A_i (U_{xi}/d_{zi} + U_{yi}/d_{zi}))/ \sum \rho_i A_i \quad (32)$$

$$\vartheta x = (\sum \rho_i A_i (U_{zi}/ (|y_i - y_c|))/ \sum \rho_i A_i \quad (33)$$
$$\vartheta y = (\sum \rho_i A_i (U_{zi}/ (|x_i - x_c|))/ \sum \rho_i A_i \quad (34)$$
$$\vartheta z = (\sum \rho_i A_i (U_{xi}/(|y_i - y_c|) + U_{yi}/(|x_i - x_c|)))/ \sum \rho_i A_i \quad (35)$$

The complete set of congruency equations is:

$$u_{cm\text{-}x} = (\sum \rho_i A_i U_{xi})/ \sum \rho_i A_i \quad (36)$$
$$v_{cm\text{-}y} = (\sum \rho_i A_i U_{yi})/ \sum \rho_i A_i \quad (37)$$
$$w_{cm\text{-}z} = (\sum \rho_i A_i U_{zi})/ \sum \rho_i A_i \quad (38)$$
$$\vartheta x = (\sum \rho_i A_i (U_{zi}/ (|y_i - y_c|))/ \sum \rho_i A_i \quad (39)$$
$$\vartheta y = (\sum \rho_i A_i (U_{zi}/ (|x_i - x_c|))/ \sum \rho_i A_i \quad (40)$$
$$\vartheta z = (\sum \rho_i A_i (U_{xi}/(|y_i - y_c|) + U_{yi}/(|x_i - x_c|)))/ \sum \rho_i A_i \quad (41)$$

The advantages of this formulation can be summarized as follows:

- There is no need to define the integral function ω and χ.
- The equations have a light mathematical structure.
- The equations are valid for 6/8/10/N degree-of-freedom one-dimensional beam model.

The limitations of this formulation can be summarized as follows:

- It is assumed that the beam thickness is much smaller than the beam length.
- It is assumed that there is no sudden change of geometry in the proximity of the interfacing cross section 1D-3D.

5.5 Validation method of the congruency equations

The validation phase have been based on the comparison of the deformation status of the central cross section of a cantilever shell-like beam, with the deformation status of the central cross section of the relative hybridized beam, see table 1 and figure 50, under bending and torsional loads.

The target of the validation is to prove that the displacement vectors (u, v, w, θx, θy, θz) of the connecting node of the hybrid structure coupled according to the equations 36-41 is exactly equal to the displacements of the virtual centre of mass of the shell-like beam in bending and torsion conditions.

In case of bending the key values to be compared, are the vertical displacement of the Cm_y and the axial rotation at the Cm_{rx}. Please refer to table 1 to see how the values have been compared in case of bending. In case of torsion the key value to be compared, is the axial rotation of the beam axis, **rz**.

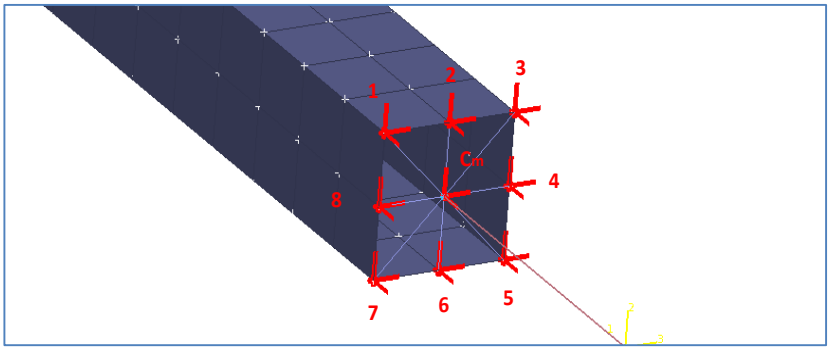

Figure 50 Hybrid cross section evaluated during the validation phase

shell-like								hybrid							
Vertical force								Vertical force							
		displacement vectors								displacement vectors					
node id		x	y	z	rx	ry	rz	node id		x	y	z	rx	ry	rz
1001G		-4,45E-04	-7,81E-02	1,35E-02	2,75E-03	-1,72E-05	-5,32E-05	1001G		-3,15E-04	-7,82E-02	1,36E-02	2,70E-03	-1,36E-05	-4,45E-04
1002G		-7,12E-04	-7,83E-02	1,34E-02	2,75E-03	-7,39E-06	-2,24E-06	1002G		-7,13E-04	-8,05E-02	1,33E-02	3,16E-03	8,28E-06	-1,54E-04
1003G		-9,80E-04	-7,81E-02	1,36E-02	2,75E-03	-7,74E-06	5,40E-05	1003G		-1,13E-03	-7,83E-02	1,37E-02	2,74E-03	-9,10E-06	4,96E-04
1004G		-7,04E-04	-7,80E-02	1,60E-04	2,72E-03	-1,40E-05	5,56E-05	1004G		-6,33E-04	-7,80E-02	1,60E-04	2,68E-03	-1,12E-05	-1,84E-04
1005G		-4,28E-04	-7,81E-02	-1,33E-02	2,75E-03	-1,96E-05	5,38E-05	1005G		-2,87E-04	-7,83E-02	-1,34E-02	2,72E-03	-1,28E-05	4,34E-04
1006G		-6,96E-04	-7,83E-02	-1,33E-02	2,75E-03	-1,52E-05	-2,08E-06	1006G		-6,91E-04	-8,01E-02	-1,31E-02	3,07E-03	-1,62E-05	-1,32E-06
1007G		-9,63E-04	-7,81E-02	-1,34E-02	2,75E-03	-1,04E-05	-5,34E-05	1007G		-1,09E-03	-7,82E-02	-1,36E-02	2,73E-03	-1,80E-05	-4,42E-04
1008G		-7,04E-04	-7,80E-02	2,12E-05	2,72E-03	-1,39E-05	-5,13E-05	1008G		-7,10E-04	-7,80E-02	2,29E-05	2,68E-03	-8,75E-06	1,80E-04
1050G		-8,46E-04	-7,82E-02	1,35E-02	2,74E-03	-2,14E-05	2,51E-05	1050G		-9,42E-04	-7,99E-02	1,34E-02	3,04E-03	-6,04E-05	5,51E-04
average		-7,20E-04	-7,81E-02	1,58E-03	2,74E-03	-1,41E-05	2,91E-06	average		-7,24E-04	-7,88E-02	1,58E-03	2,84E-03	-1,58E-05	4,83E-05
rms		1,95E-04	1,01E-04	1,25E-02	1,28E-05	4,93E-06	4,71E-05	rms		3,00E-04	1,01E-03	1,25E-02	1,94E-04	1,84E-05	3,87E-04
cross-check		-7,20E-04	-7,81E-02	1,58E-03	2,74E-03	-1,41E-05	2,91E-06	cross-check		-7,24E-04	-7,88E-02	1,58E-03	2,84E-03	-1,58E-05	4,83E-05
average α (grad)					3,52E-00	-1,81E-02	3,74E-03	average α (grad)							
Cm Hybrid (node 24)								Cm Hybrid		-6,98E-04	-7,87E-02	8,91E-05	2,69E-03	-1,24E-04	-2,90E-07

Table 1 Comparison of the deformation status of the cross-section of the shell-like vs the hybrid beam

In order to prove the validity and the global application of the congruency equations, they have been tested as following:

- 4 different cross sections with square, circular, C and arbitrary (abc) cross sectional shape, with homogeneous distribution of the mesh and homogeneous distribution of the thickness have been compared, the hybrid model versus the shell-like model, under 2 different load cases, bending and torsion.
- 4 different cross sections with square, circular, C and arbitrary (abc) cross sectional shape, with non-homogeneous distribution of the mesh and homogeneous distribution of the thickness have been compared, the hybrid model versus the shell-like model, under 2 different load cases, bending and torsion.
- 4 different cross sections with square, circular, C and arbitrary (abc) cross sectional shape, with homogeneous distribution of the mesh and non-homogeneous distribution of the thickness have been compared, the hybrid model versus the shell-like, under 2 different load cases, bending and torsion.

In the first phase of the validation, a total of 24 beams (hybrid and shell-like) have been tested under 48 study-cases (bending and torsion). An overview of all the hybrid beams tested versus the respectively shell-like version, is given in figure 51.

As cross-check, based on a single beam, with squared sections, with non-homogeneous distribution of the mesh and non-homogeneous distribution of the thickness have been done, hybrid versus shell-like, under two different load cases bending and torsion, providing errors below 2% in all conditions.

Finally, in order to check the error sensitivity to the number of nodes of the interfacing cross sections, a second validation phase has been done, starting from the cross sections with homogenoeus mesh and densitiy distribution, increasing the number of nodes up to a factor three, and comparing them with the relative shell-like derived beams.

The validation phase is reported in the following chapter 6.

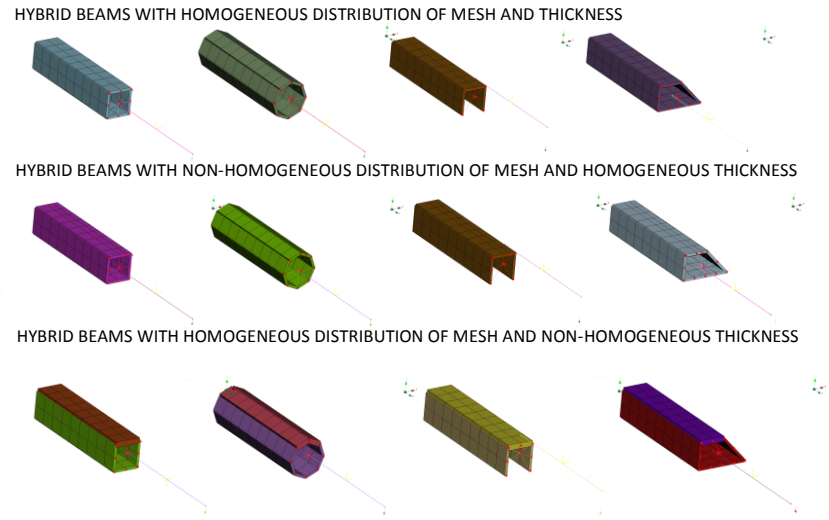

Figure 51 Hybrid beams tested in the validation phase

6 VALIDATION PHASE

In this chapter the validation approach of the congruency equations for the rigorous connection of dissimilar FEM elements is presented. In the first part all the features of the tested beams and the relevant informations of the test conditions are reported, in the second part the results are presented. Finally the conclusions and recommendations are given.

6.1 Characterization of the beams and test conditions

In the first phase of the validation, four thin-walled shell-like beams with homogeneous distribution of mesh and density have been created, the beams differentiate between each other only from their cross-section shape; the cross-section selected are as follows:

- Squared
- Circular
- Arbitrary
- C-shape

Starting from those four beams, additional eight beams have been created:

- four shell-like beams with homogeneous distribution of mesh and non-homogeneous thickness distribution
- four shell-like beams with non-homogeneous distribution of mesh and homogeneous thickness distribution

A total of twelve shell-like beams have been created, starting from these twelve beams, the relative hybrid beams have been created and compared.

In the second phase of the validation, the error sensitivity analysis has been performed based on the a set of shell-like beams with homogeneous mesh and density distributions of beams, increasing the number of nodes up to a factor three of the interfacing cross section. Each beam has been constrained on one side (cantilever beam), and then loaded on the free end, alternatively with vertical forces or moments producing bending and torsion. The congruency equations have been implemented through a multi-point constraints elements with a semi-automated tool. In order to derive to the hybrid version, the shell-like beam has been split longitudinally in two parts, and one of the part has been substitute with a mono-dimensional beam with arbitrary cross section. For the non-homogenous mesh distribution test, an asymmetrical mesh has been realized, while for the non-homogeneous density distribution test, two set of shell-like elements have been set to a double value of density.

In the following sub-paragraph all the characteristic of the tested beams are reported.

6.1.1 Beam with squared section

The shell-like beam with squared cross section has the following geometrical characteristic:

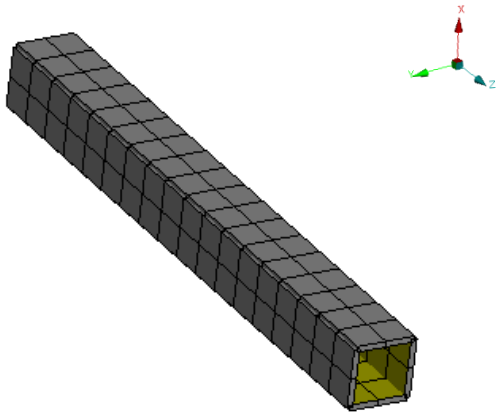

Figure 52 shell-like beam with square cross-section

C.O.G. Cartesian coordinates- x,y,z- (mm)	5	5	50

INERTIA TENSOR		
0.0470275	6.51128e-15	9.566e-10
6.51128e-15	0.0471537	-7.65863e-09
9.566e-10	-7.65863e-09	0.00203259

PRINCIPAL INERTIAS		
0.0471537	0	0
0	0.0470275	0
0	0	0.00203259
PRINCIPAL DIRECTIONS		
5.97152e-06	-1	3.17092e-07
1	5.97487e-06	-2.66262e-07
2.6626e-07	3.17093e-07	1

6.1.2 Beam with circular section

The shell-like beam with circular cross section has the following geometrical characteristic

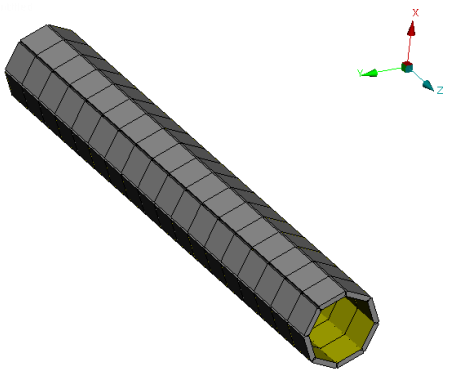

Figure 53 shell-like beam with circular cross-section

C.O.G. Cartesian coordinates - x,y,z – (mm)	5	5	50

INERTIA TENSOR		
0.0293448	-1.70109e-11	3.13613e-10
-1.70109e-11	0.0293448	-4.20339e-09
3.13613e-10	-4.20339e-09	0.00169897

PRINCIPAL INERTIAS		
0.0293448	0	0
0	0.0293448	0
0	0	0.00169897
PRINCIPAL DIRECTIONS		
0.707109	0.707105	-0.000114511
-0.707105	0.707109	-2.42632e-10
8.09716e-05	8.09715e-05	1

6.1.3 Beam with C section

The shell-like beam with C cross section has the following geometrical characteristic

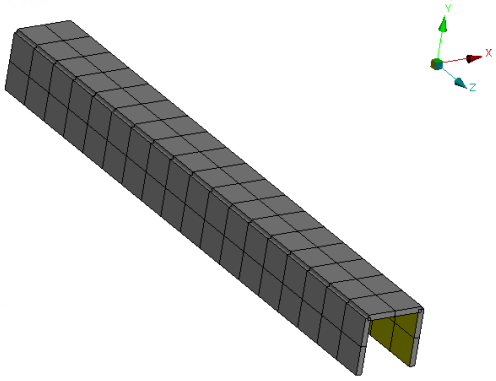

Figure 54 shell-like beam with C cross-section

C.O.G. Cartesian coordinates - x,y,z – (mm)	5	6.66667	50

INERTIA TENSOR		
0.0200732	3.25477e-15	4.00822e-10
3.25477e-15	0.0202368	-3.82931e-09
4.00822e-10	-3.82931e-09	0.000817708

PRINCIPAL INERTIAS		
0.0202368	0	0
0	0.0200732	0
0	0	0.000817708
PRINCIPAL DIRECTIONS		
1.76982e-06	-1	1.64398e-07
1	1.76951e-06	-1.11832e-07
1.11832e-07	1.64399e-07	1

6.1.4 Beam with arbitrary cross section

The shell-like beam with arbitrary cross section has the following geometrical characteristic

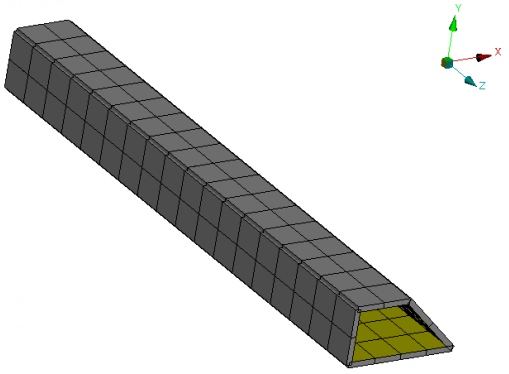

Figure 55 shell-like beam with arbitrary cross-section

C.O.G. Cartesian coordinates - x,y,z - (mm)	8.535	4.076	50

INERTIA TENSOR		
0.036426	0.0003925	3.61091e-09
0.0003925	0.0376299	-4.05029e-09
3.61091e-09	-4.05029e-09	0.00278268

PRINCIPAL INERTIAS		
0.0377466	0	0
0	0.0363093	0
0	0	0.00278268
PRINCIPAL DIRECTIONS		
0.284907	0.958555	1.07185e-07
0.958555	-0.284907	-1.16974e-07
-8.15883e-08	1.3607e-07	-1

6.1.5 Error sensitivity analysis beams

To study the deviation of the error depending on the number of nodes of the interfacing cross sections, shell-like beams with higher number of nodes per cross-section have been created, respectively square, circular, C and arbitrary cross-sections. The nodes for each beams have been incremented first of a factor 2, then of a factor 3, see figure 58.

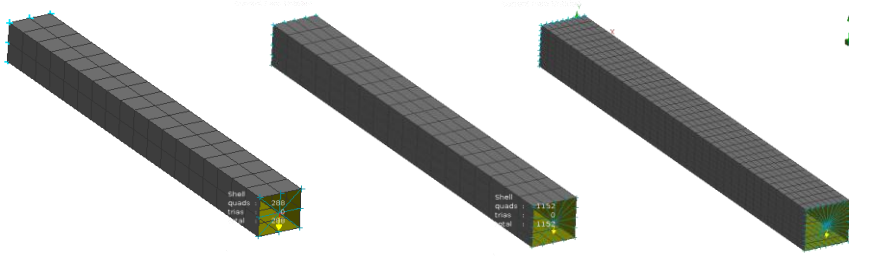

factor 1 factor 2 factor 3

Figure 56 Error sensitivity analysis beams

6.2 Results

In this paragraph the results of the comparison between shell-like and hybrid beams, according to the method described in paragraph 5.6, is reported.

The results are reported in two parts form, the first part, from figure 59 to figure 64 refers to the beams with constant number of nodes, thickness and mesh distribution is then modified. The second part, from figure 65 to figure 68, refers to the beams with mesh and density constant, whereby the number of nodes is then varied.

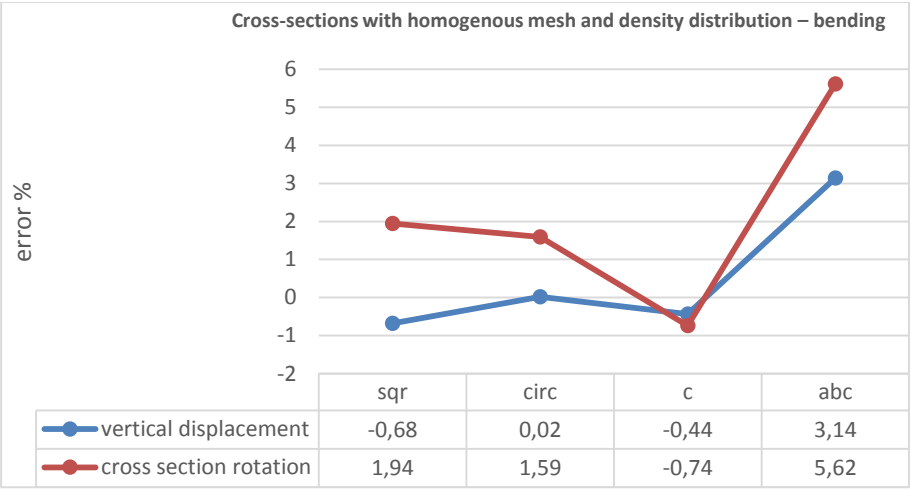

Figure 57 Cross-sections with homogenous mesh and density distribution – bending

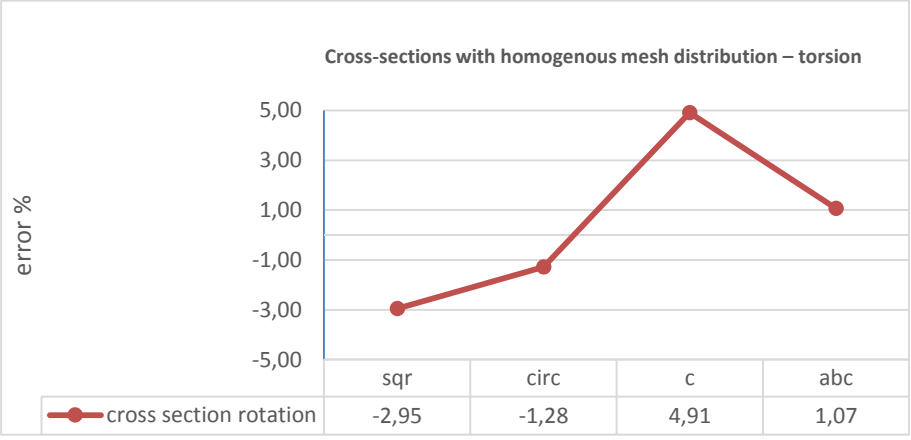

Figure 58 Cross-sections with homogenous mesh and density distribution – torsion

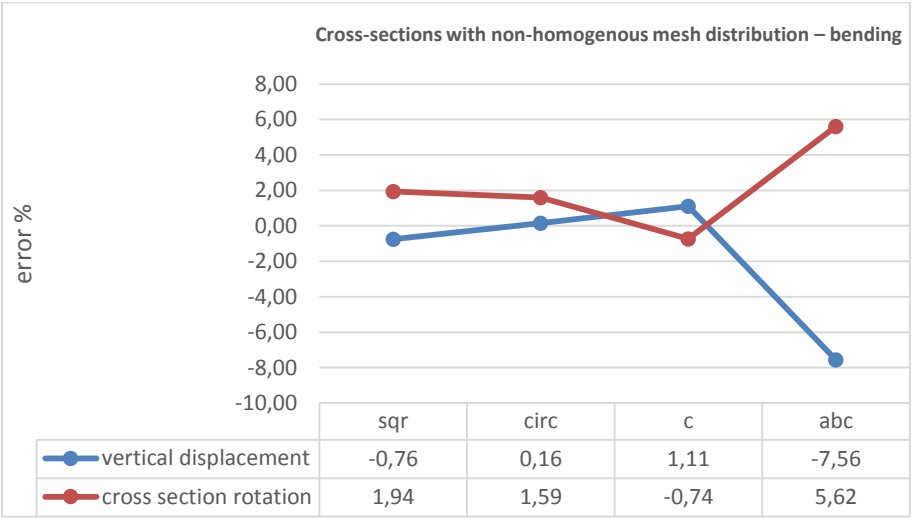

Figure 59 Cross-sections with non-homogenous mesh distribution – bending

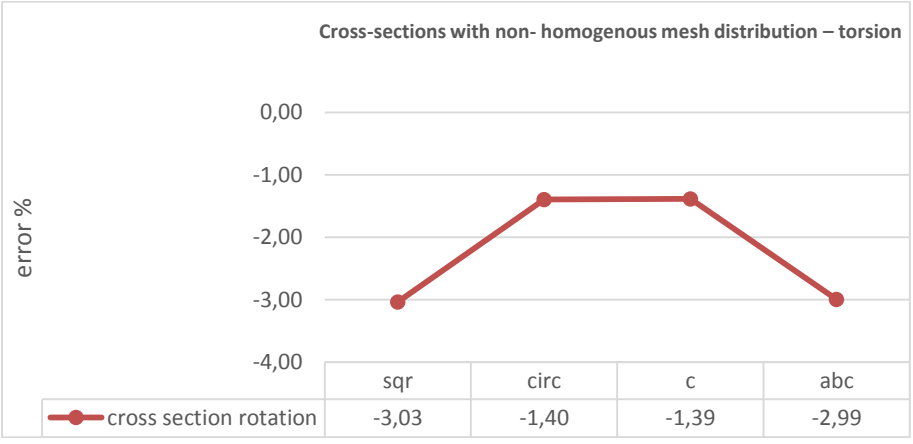

Figure 60 Cross-sections with non-homogenous mesh distribution – torsion

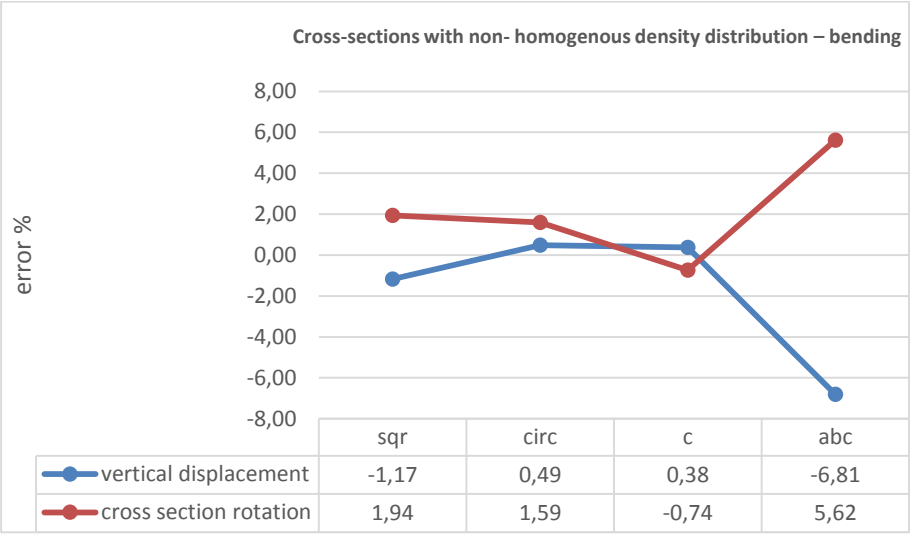

Figure 61 Cross-sections with non-homogenous density distribution – bending

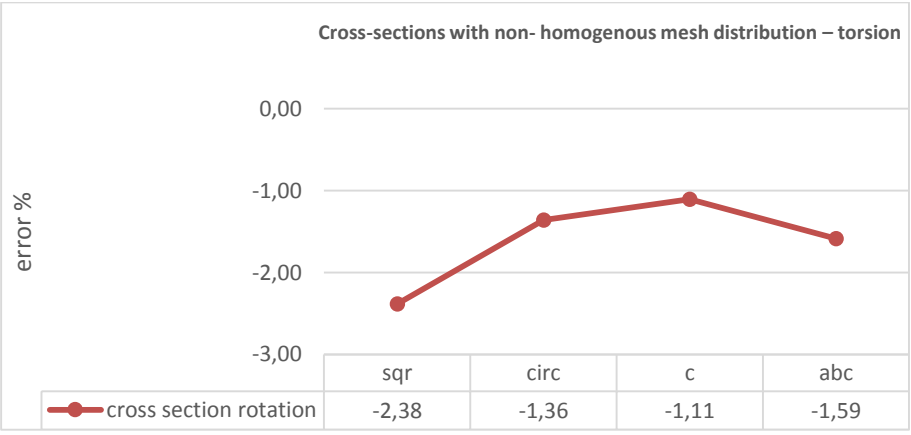

Figure 62 Cross-sections with non-homogenous density distribution – torsion

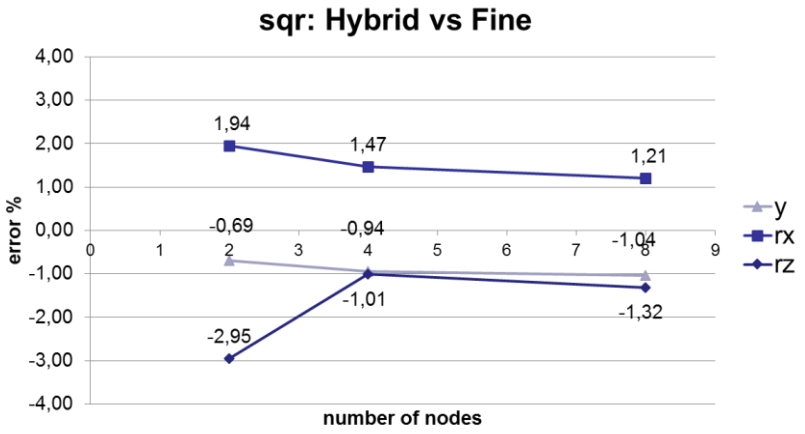

Figure 63 Cross-sections with higher number of nodes – squared section

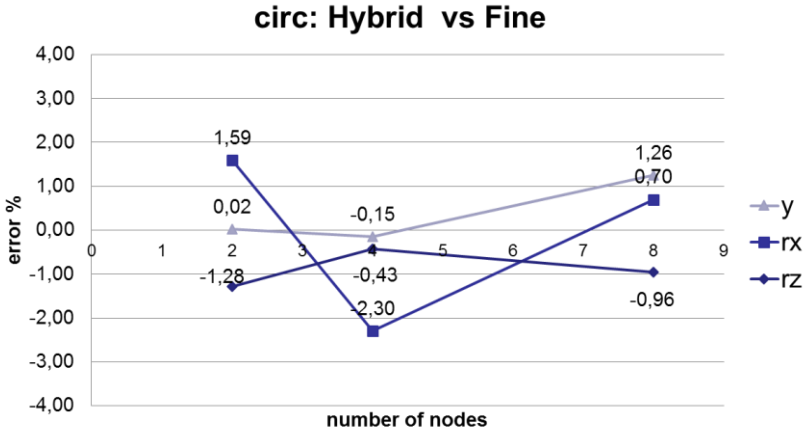

Figure 64 Cross-sections with higher number of nodes – circular section

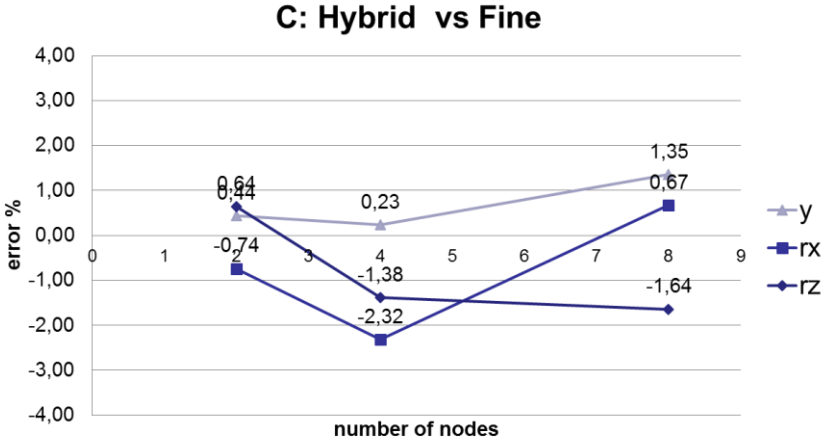

Figure 65 Cross-sections with higher number of nodes – C section

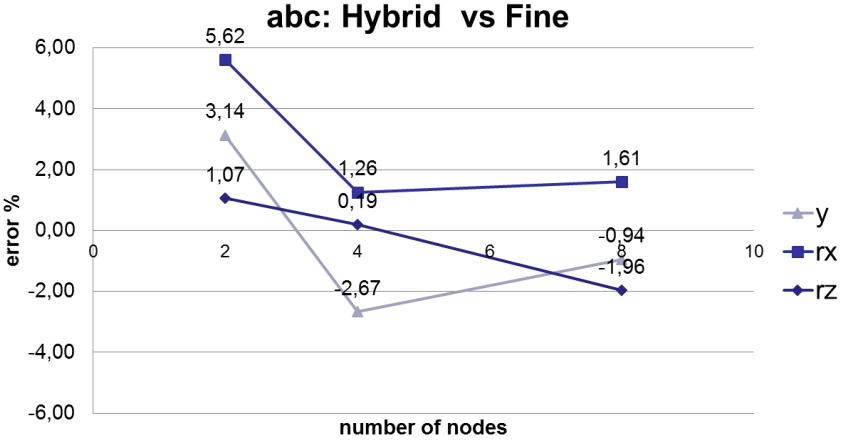

Figure 66 Cross-sections with higher number of nodes – abc section

6.3 Conclusions and recommendations

The beams with square, circular and C cross-sections present in all conditions an average error below 2%. The error is also not sensitive to the number of nodes, this implies that the congruency equations are independent from the number of nodes of the cross section and that can be applied to structures with large number of nodes. The error related to the beams with the arbitrary cross section is higher than expected, above 5%, however the error sensitivity of those beams result very high, increasing the number of nodes the average error drops again below 2%. This circumstance can be explained considering that the arbitrary cross section has a complex shape, a borderline ratio length/width for the application of the Timoshenko equations and a number of nodes, equal to 10, too low to precisely describe the in plane and out-of plane deformations of the arbitrary cross section, thus augmenting the number of nodes of the cross sections of a factor two or more, it is possible to achieve the same performance of the other cross sections.

All in all an average error of 2% is a very good result for concept modelling applications, whereby the error is always above 3%. However an error in average below 1% would have been expected, a deeper analysis of the results shows that part of the error detected is due to some mathematical singularities that appear in certain conditions. When the nodes are positioned on the inertia axes of the cross sections, the equations present a singularity (denominator equal zero) and this, translated in FEM applications, increases the overall error of about 1% (in average). In order to reduce the error, it is recommended to avoid to set nodes on the inertia axes. As evidence of what above stated the beam of figure 50 has been re-modelled as in figure 67 in order to avoid such condition, the error in bending condition dropped form 0.7 % to 0.05%.

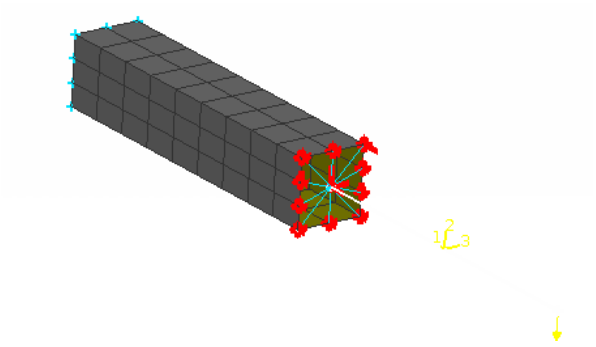

Figure 67

7 INTEGRATION OF THE HYBRID CONCEPT MODEL IN THE OPTIMIZATION SEQUENCE

This final chapter presents a real application of a multi-objective optimization sequence of a complete car body, based on a hybrid concept model and morphing applications. The aim is to illustrate how the implementation has been undertaken and the capabilities of the hybrid concept model combined with the solutions presented within the framework of this dissertation.

7.1 Integration of the model

One of the goal of this research activity is to create a concept model based on hybrid structures achieving static and dynamic performance ideally equal to the fine FE shell model (reference model), which can be integrated in a multi-objective optimization sequence and post-processing software [16].

In order to achieve this target several engineering challenges have been tackled and relative solutions proposed:

- Insuring consistent stress calculation between the detailed shell-like structure and the one-dimensional beams (linearized-crash case).
- Defining suitable connecting elements between the detailed shell-like structure for the joint and the interfacing mono-dimensional beam structure.

- Defining the most suitable morphing-box shape and related morphing/optimization parameters.

However implementing those solutions in a multi-objective optimization sequence of a complete car body, whereby pre and post processing semi-automated tools play a relevant role, is not an obvious task.

In order to gain the necessary know-how, the first investigations of the optimization sequences, static and dynamic, have been based on simple structures, extending the investigation to more complex structures up to the complete hybrid BiW. The complete implementation process is represented figure 68.

The implementation process begins studying the stress and deformation status of hybrid cantilever beams, identifying a homogeneous stress calculation approach, defining the stress item codes (item codes are integer numbers assigned to an element, for specific output quantities such as the major principal stress or Von Mises stress formulation). Then simplified joint structures have been investigated in order to validate the selected stress codes and above all, to define the best connecting elements and morphing strategy.

Finally the selected items codes, the connecting elements and the morphing-boxes, have been implemented in the full vehicle.

Proceeding step by step with the implementation of the different solutions proposed, it has been possible to define carefully all the requirements of pre and post processing semi-automated tools.

The most critical passages of the implementation process are:

- Integration of the morphing variables in the optimization sequence.
- Definition of the morphing vectors.
- Definition of design variable for the morphing vectors.
- Definition of traces-lines (for post-processing).
- Definition of smooth-parameters in order to limit geometrical differences between consecutive dissimilar elements.
- Definition of the areas where the application of three dimensional detailed structures are necessary.

Finally a full multi-disciplinary/objective optimization process of a hybrid concept morphed model of a complete BiW is described in the next paragraph.

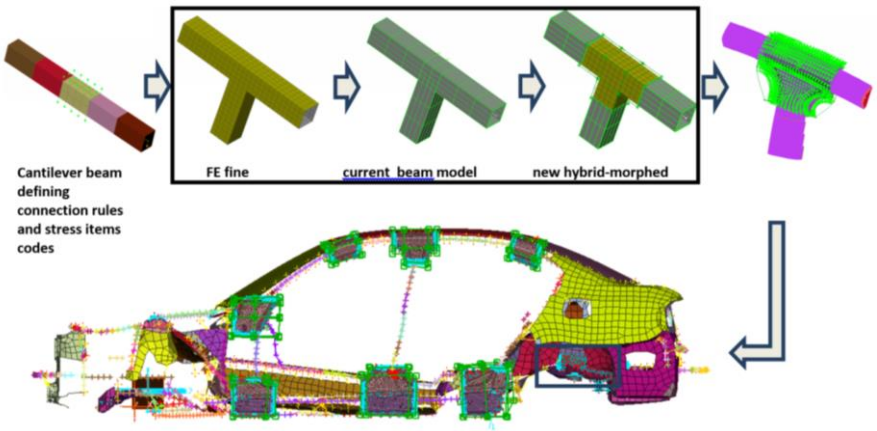

Figure 68 Implementation sequence of the Hybrid Morphing Concept Model

7.2 Optimization sequence

The next and final step of this work is the implementation and verification of the hybrid morphing approach on a full BiW multi-disciplinary optimization run, according to the BMW standard.

The first step is to create a BMW E90 hybrid morphing concept model, fourteen relevant joints have been selected from the fine model and tailored morphing boxes have been designed in order to create the deformation vectors, then the related variable cards (design variables), have been then assigned, one for each joint.

The remaining part of the concept model has been derived from the fine shell-like BiW model, using one-dimensional beams and shell panels, finally the beam, the joints and the panels have been connected using RBE2 elements.

A multi-disciplinary cost function has been implemented, including static, dynamic, roll over, NVH and pseudo-crash constraints, the objective of the optimization is to increase the Eigen-frequency of the 2nd Eigen-mode of 10% while minimizing the weight.

More than thousand design variables have been created in order to optimize the height, the width and thickness of each cross section of each beam, the thicknesses of the shell panels and the global dimension of the joints. The optimization sequence is executed by a gradient based optimizer, in the objective function a penalty method is included (so called ß-method), avoiding to stop the

optimization in case of violations of the constraints. The complete optimized body is shown in figure 69. The optimized joints have been highlighted with colors. In the pictures a detail of a morphed joint is also reported. For each joint the percentile variation of each design variable (1 variable card for each joint: scaling effect) assigned to the joints has been reported, additional congruency constraints between interfacing dissimilar cross-sections have been also introduced. The percentile variation is calculated between a nominal and a final configuration, whereby in this case the final configuration is defined using morphing boxes, increasing the height and width of the interfacing cross sections of 100% with respect of the nominal value, however any other final configuration can be freely defined, according to the targets of the optimization [16].

The results of the optimization run show how the proposed hybrid morphing concept model represents a concrete enhancement with respect of the actual concept model. The hybrid model, from one side, has the potential to assure a better accuracy and robustness (static and dynamic stiffness calculation), on the other side, provides clear indications to the designer on “what” has to be modified (which beams and joints), in order to achieve certain structural targets.

The big advantage of using hybrid model is that a wide range of important design information can be extracted, giving clear indications to the designer on “how” to modify certain structures and sub-structures, and on the feasibility of certain modifications. Once the areas, to be tackled, have been defined, more exhaustive investigations and optimizations can be launched. For example, in case that the static stiffness of a joint has to be modified, it is possible to run a detailed geometrical optimization, assigning one or more design variables to each morphing-box of the joint, see figure 70; or to include the thicknesses of the shell-elements of the internal reinforcing plates of the joints, as design variables in the optimization sequence see figure 71. Another interesting application could lead to an optimization of the joint’s stiffness of the complete car body keeping constant the rest of the geometry. The benefits of running such an optimization of joint’s stiffness, based on a hybrid morphing model and not in the actual concept model possible, lies the local accuracy of results, increasing the acceptance of the proposed modifications.

It is important to highlight that the total time for a complete multi-disciplinary optimization run of the hybridized-morphing model is not much higher than the actual concept model, the augmented calculation time linked to the increase of the number of nodes, can be estimated in some minutes for each cycle, considering that each optimization sequence is about 50 cycles, the total increase of time for a complete multi-disciplinary optimization can be estimated in a maximum of 2.5 hours (max +40%).

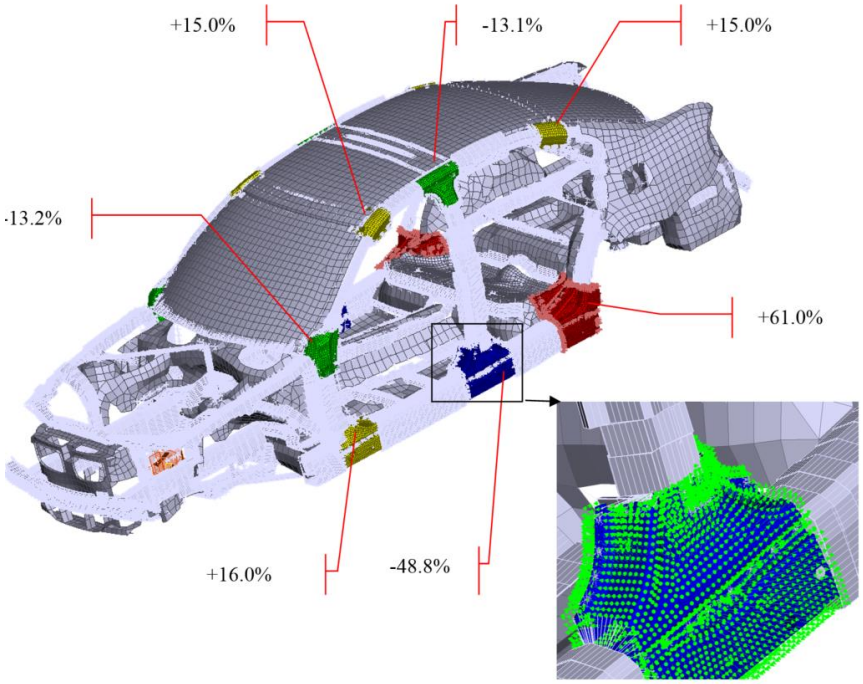

Figure 69 Optimized Hybrid Morphed concept model of a BMW E90 BiW, with percentile variation information of the geometry of the morphed joints.

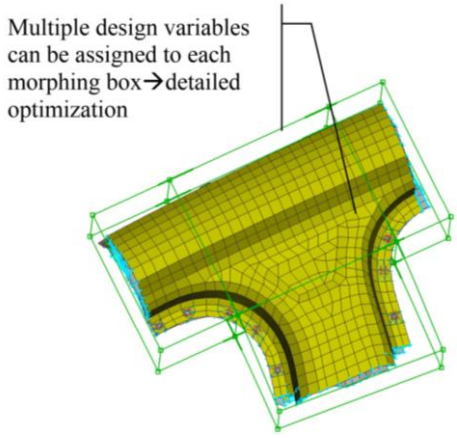

Figure 70 Joint with morphing boxes

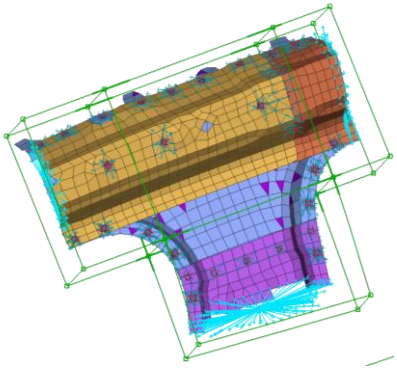

Figure 71 Internal reinforcement-plates

The “Hybrid Morphing Concept Model” shows an increase in terms of accuracy, robustness and quality of the optimization results, with respect of the actual modeling approach. The current multi-objective optimization process combined with hybrid structure and morphing applications does not show critical area.

8 CONCLUSIONS AND FINAL REMARKS

The study was set out to improve the beam and shell concept model, seeking for accuracy, robustness and new applications for multi-objective optimization sequences.

In order to achieve the proposed targets, hybrid structures and morphing applications have been introduced. Within this development process two main engineering challenges have been tackled: the homogenous stress calculation in hybrid structures and the rigorous connections of dissimilar FE elements (1D-3D). While the stress calculation can be defined merely as a “functional” challenge, the rigorous connection is a true scientific challenge. Deriving the congruency equations for connecting dissimilar FE elements through the “principle of virtual work”, a new fundamental property of the centre of mass of the thin-walled beam cross-sections has been defined. The new property of centre of mass is what the author consider the central output of this dissertation, its definition leads to a simple, universally applicable and well validated structure of a set of congruency equations.

Further developments of this work could lead to creating a software tool, to be implemented in any pre-processor program, capable of automatically employing the congruency equations between dissimilar elements for any type of cross-sections. Minor aspects like avoiding mathematical singularities in the implementation phase of the equations would have to be investigated.

The set of congruency equations for the rigorous connection of dissimilar FEM elements for hybrid (car body) thin-walled structures, built on the “principle of virtual work” and the fundamental property of the center of mass, can be considered a true enhancement in the concept modeling field.

More in details this study started with a deep review of the “beam and shell” model, analyzing and tackling through a problem solving approach the critical areas of the concept modeling design process.

The first step was to define the gap between the expected modeling error (ideally equal zero) and the actual modeling error in static and dynamic conditions, breaking down the error and confirming the dominant position of the joint modeling. Having acknowledged the key role of the joint modeling and its lack of performance

in terms of accuracy and robustness, a research study to define the relevant prior art in the field of joint modeling has been carried out.

In order to meet the modeling expectations, a completely new joint modeling solution have been proposed and developed within this research activity. The solution is based on the implementation of joint hybrid structures, whereby the mono-dimensional elements are coupled with three dimensional structures (formed by 2D elements).

The idea behind the hybridization is quite simple, the lack of accuracy and robustness of a model is overcome by introducing more information to the detriment of the calculation time. However the implementation of hybrid structures is not trivial, three main challenges are reckonable: to avoid loss of optimization variables, to realize homogeneous stress calculation between interfacing dissimilar elements, to define “zero” error connections between interfacing dissimilar elements.

The first subject has been tackled introducing well known morphing techniques, the contribution of the author in this area concerns the definition of the “best” morphing box shape in order to avoid structural congruency issues (e.g. overlapping of cross-sections, etc..), the selection of the most appropriate morphing technique for the integration of the variable in the multi-objective optimization sequence and the selection of the optimization variables.

The homogenous stress calculation between dissimilar FEM elements, has been realized analyzing of the theoretical background of the FEM elements, the main contribution of the author in this area concerns the definition of the parameters and the validation method.

The definition of rigorous connections between dissimilar FEM elements is clearly the central objective and the main scientific challenge of this research activity. The problem has been tackled once more through a problem solving loop, setting targets, defining gaps (actual vs target situation), searching for “prior art” , defining the “state of the art”, benchmarking all the possible solutions, root cause analysis and identifying the critical aspects of each solution.

The solution proposed by “Kim&Kim” based on the “principle of virtual work” clearly represents the so called “state of the art” approach for the rigorous connection of dissimilar elements, however two negative aspects characterize this solution, first the complexity of the solution itself and second the limited range of validity, indeed this solution is defined just for a limited number of specific cross–sections.

In order to overcome those drawbacks, a new solution has been developed and proposed within this research activity.

Defining a new system of equations for the rigorous connection of dissimilar elements, a new fundamental property of the centre of mass of the beam cross-sections has been identified.

Applying this property of centre of mass and the “principle of virtual work” a new system of equations for the rigorous connection of dissimilar FEM elements have been described, the efficacy of the system of equations have been then proved.

Finally in order to verify the suitability for real world applications, all the solutions developed during this research activity have been implemented and tested in a multi-objective optimization sequence with a positive outcome.

The main achievements of this dissertation from a scientific point of view can be summarized as follows:

- Definition of a new fundamental property of the centre of mass of the thin-walled beam cross-sections.
- Definition of a set of of congruency equations for the rigorous connection of dissimilar FEM elements for hybrid thin-walled structures, whereby one-dimensional elements are coupled with three-dimensional joint structures, applicable without any limitation linked to cross sectional shape of number of DOF of the mono-dimensional beam model.
- Definitions of a validation method for congruency equations

The main achievements of this dissertation from an industrial point of view can be summarized as follows:

- Definition of a “hybrid morphed concept model” with higher accuracy and robustness capable of being integrated in a multi-objective/disciplinary optimization sequence.
- Definition and method thereof of a homogenous stress calculation approach between dissimilar FEM elements.
- Definition and method thereof of a new precise connecting FEM element with the potential of being integrate in a pre-processor software.

List of figures

List of tables

Bibliography

1. **www.vecom.org. [Online] 2008. www.vecom.org.**

2. ***Numerische Strukturoptimierung mit Balken-Schalen-Modellen.*** **Cremers, L., Schneeweiss, H. und Kroiss, M. Landshuter Leichtbau Colloquium : s.n., 2007.**

3. ***Shape Optimization with MSC.NASTRAN.*** **Irrgang , A. und Raasch, I. MSC.NASTRAN, European User's Conference : s.n., 1988.**

4. ***NVH Structural Optimization using Beams and Shells FE Concept Models in the early Car Development Phase at BMW.*** **Moroncini, A., Cremers, L. und Kroiss, M. Leuven : ISMA 2010, 2010.**

5. ***Car body concept modeling for NVH optimization in the early design phase at BMW: a critical review and new advanced solutions.*** **Moroncini, A., Cremers, L. und Baldanzini, N. Leuven ISMA 2012 : s.n., 2012.**

6. ***Evaluation of optimization algorithms for crash and NVH.*** **Duddeck, F. und Volz, K. s.l. : Elsevier, 2005, Bd. Computational fluid and solid mechanics.**

7. ***Multidisziplinäre Optimierung im Produktentwicklungsprozess der Automobilindustrie - Dudeck.*** **Duddeck, F. s.l. : Weimarer optimierungs und stochastiktage, 2005.**

8. Math Works. ***MATLAB User's guide.*** **2012.**

9. ***Multiobjective Optimization and Control.*** **G.P.Liu, J.B.Yang. 2003.**

10. ***Multi-objective optimization using genetic algorithms: A tutorial.*** **A. Konak, D.B.Coit, A.E. Smith. 91, s.l. : Elsevier, 2006, Bd. Reliability engineering and system safety.**

11. ***A vehicle body concept modeling approach using reduced models of beams, joints and panels.*** **Stigliano G., Mundo D. , Donders S. Paris : "ECCM 2010 - IV European Conference on Computational Mechanics", 2010.**

12. N., Bylund. ***Simulation driven product development applied to car body design.*** **Lulea : s.n., 2004.**

13. ***Numerical approximation of vehicle joint stiffness by using responce surface method.*** **S.B. Lee, J.R. Park, H.J. Yim. s.l. : International journal of automotive technology, 2003, Bd. 3.**

14. ***Major compliance joint modelling survey for automotive body structures.*** **M, Shahhosseini Ali. Indiana State University USA : s.n., 2010, Bd. International journal vehicle system modelling and testing.**

15. BETA CAE. ***ANSA Users Guide.*** **2012.**

16. MSC. ***Nastran User's Guide.*** **s.l. : MSC, 2010.**

17. ***A one-dimensional theory of thin-walled curved rectangular box beams under torsion and out-of-plane bending.*** **Kim, Yoon Young und Kim, Youngkyu. 2002, Bd. International journal for numerical methods in engineering.**

18. ***Analysis of thin-walled closed beams with general quadrilateral cross sections.*** **Kim, Yoon Young und Kim, Youngkyu. s.l. : ASME, 1999, Bd. 66.**

19. ***Analysis of thin-walled curved box beam under in-plane flexure.*** **Kim, Y. und Kim, Y. Y. s.l. : Elsevier, 2003, Bd. International journal of solids and mechanics.**

20. ***Fully coupled 10-degree-of-freedom beam theory for piecewise straight thin-walled beams with general quadrilateral cross sections.*** **Jang, G.W. und Kim, Y.Y. s.l. : ASCE, 2010, Bd. Journal of structural engineering.**

21. ***Hat interpolation wavelet-based multi-scale Galerkin method for thin-walled box beam analysis.*** **Kim, Y.Y. und Jang, G. W. 2002, Bd. International journal for numerical methods in engineering.**

22. ***Higher order in-plane bending analysis of box beams connected ant an angled joint considering cross-sectional bending warping and distortion.*** **47, Seoul : Elsevier , 2009, Bde. Thin-walled structures.**

23. ***Higher-order beam analysis of box beams connected at angled joints subjected to out-of-plane bending and torsion.*** **Jang, G.W., Kim, K. J. und Kim, Y.Y. 75, s.l. : Wiley Interscience, 2008, Bd. International journal for numerical methods in engineering .**

24. ***Mixed state-vector finite element analysis for a higher-order box beam theory.*** **Jang, G. W. und Kim, Y. Y. 36, s.l. : Springer Verlag , 2005, Bd. Comput Mech.**

25. ***New accurate efficient modeling techniques for the vibration analysis of T-joint thin-walled box structures.*** **Kim, J.H., et al. 39, s.l. : Elsevier, 2002, Bd. International journal of solids and structures.**

26. ***One-dimensional analysis of thin-walled closed beams having general cross-sections.*** **Kim, J. H. und Kim, Y. Y. 49, s.l. : John Wiley and Sons, 2000, Bd. International journal for numerical methods in engineering.**

27. ***Significance of distortion in thin-walled closed beam section design.*** **Heo, S., Kim, J. H. und Kim, Y. Y. 40, s.l. : Elsevier, 2003, Bd. International journal of solids and structures .**

28. ***Theoretical analysis of coupled torsional warping and distortional waves in a straight thin-walled box beam by higher order beam theory.*** **Jang, G.W. und Kim, Y.Y. 330, s.l. : Elsevier, 2011, Bd. Journal of sounds and vibration.**

29. ***Thin-walled closed box beam element for static and dynamic analysis.*** **Kim , Y. Y. und Kim, J. H. . 45, s.l. : John Wiley and Sons, 1999, Bd. International journal for numerical methods in engineering.**

30. ***Thin-Walled Multicell Beam Analysis for Coupled Torsion, Distortion, and Warping Deformations.*** **Kim, J. H. und Kim, Y. Y. s.l. : ASME, 2001, Bd. 68.**

31. ***Topology optimization of beam cross sections.*** **Kim, Y.Y. und Kim, T. S. 37, s.l. : Elsevier, 1998, Bd. International journal of solids and structures.**

32. ***Vibration analysis of piecewise straight thin-walled box beams without using artificial joint springs.*** **Jang, G.W und Kim, Y.Y. 326, s.l. : Elsevier, 2009, Bd. Journal of sounds and vibration.**

33. Gjelsvik, A. ***The theory of thin walled bars.*** **1981.**

34. ***RTYPE Elements.*** **MSC Software Corporation. 2011, Bd. NAS101B.**

35. ***Coupling 1D beams to 3D bodies.*** **Mc Court, D, et al. Belfast : s.n.**

36. ***Mixed dimensional coupling in finite element stress analysis.*** **K.W., Shim, Monaghan, D und Armstrong, C. G. Belfast : s.n.**

37. ***Timoshenko beams.*** **Haukaas, T. s.l. : University British Columbia.**

38. ***A comparative evaluation of genetic and gradient-based algorithms applied to aerodynamic optimization .*** **D.W. Zingg, M. Nemec, T.H. Pulliam. 17, s.l. : REMN, 2008, Bd. Shape design in aerodinamics.**

39. ***Energy Principles in Structural Mechanics.*** **Tauchert, T.R. s.l. : McGraw-Hill, 1974.**

40. ***Shape and size optimization of an engine suspension system.*** **N. Baldanzini, A. Scippa. Leuven : ISMA2004, 2004.**

41. ***Designing the dynamic behaviour of an engine suspension system through genetic algorithms.*** **N. Baldanzini, D. Caprioli, M. Pierini. s.l. : ASME, 2001, Bd. 123.**

42. ***An improved method for updating simplified finite elements models of mechanical systems.*** **N. Baldanzini, P. Citti, M. Pierini. s.l. : IPC2001T348, 2001.**

43. H., Song. ***Rigorous joining of advanced reduced-dimensional beam models to 3D finite elements models.*** **2010.**